Orally administrated chitosan microspheres bind Helicobacter pylori and decrease gastric infection in mice

Patrícia C Henriques, Lia M Costa, Catarina L Seabra, Bernardo Antunes, Ricardo Silva-Carvalho, Susana Junqueira-Neto, André F Maia, Pedro Oliveira, Ana Magalhães, Celso A Reis, et al.

Journal Pre-proof

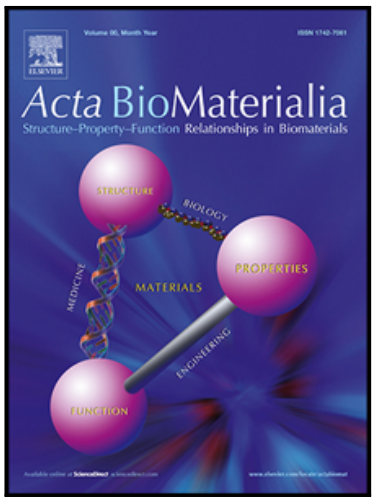

Orally administrated chitosan microspheres bind Helicobacter pylori and decrease gastric infection in mice

Patrícia C. Henriques , Lia M. Costa , Catarina L. Seabra , Bernardo Antunes , Ricardo Silva-Carvalho , Susana Junqueira-Neto , André F. Maia , Pedro Oliveira , Ana Magalhães , Celso A. Reis , Fátima Gartner , Eliette Touati , Joana Gomes , Paulo Costa , M.Cristina L. Martins , Inês C. Gonçalves

PII: S1742-7061(20)30365-2
DOI: https://doi.org/10.1016/j.actbio.2020.06.035
Reference: ACTBIO 6797

To appear in: *Acta Biomaterialia*

Received date: 20 December 2019
Revised date: 22 June 2020
Accepted date: 25 June 2020

Please cite this article as: Patrícia C. Henriques , Lia M. Costa , Catarina L. Seabra , Bernardo Antunes , Ricardo Silva-Carvalho , Susana Junqueira-Neto , André F. Maia , Pedro Oliveira , Ana Magalhães , Celso A. Reis , Fátima Gartner , Eliette Touati , Joana Gomes , Paulo Costa , M.Cristina L. Martins , Inês C. Gonçalves , Orally administrated chitosan microspheres bind Helicobacter pylori and decrease gastric infection in mice, *Acta Biomaterialia* (2020), doi: https://doi.org/10.1016/j.actbio.2020.06.035

Orally administrated chitosan microspheres bind Helicobacter pylori and decrease gastric infection in mice

Patrícia C. Henriques [a,b], Lia M. Costa [b], Catarina L. Seabra [a,b,c], Bernardo Antunes [b], Ricardo Silva-Carvalho [b], Susana Junqueira-Neto [a,c], André F. Maia [a,d], Pedro Oliveira [e], Ana Magalhães [a,c], Celso A. Reis [a,c,e,f], Fátima Gartner [a,c,e], Eliette Touati [g], Joana Gomes [a,c], Paulo Costa [h], M. Cristina L. Martins [a,b,e], Inês C. Gonçalves [a,b*]

[a] i3S - Instituto de Investigação e Inovação em Saúde, Universidade do Porto, Rua Alfredo Allen, 208, 4200-135 Porto, Portugal

[b] INEB - Instituto de Engenharia Biomédica, Universidade do Porto, Rua Alfredo Allen, 208, 4200-135 Porto, Portugal

[c] IPATIMUP – Institute of Molecular Pathology and Immunology of the University of Porto, Rua Dr. Roberto Frias s/n, 4200-465 Porto, Portugal

[d] IBMC – Instituto de Biologia Molecular e Celular, Universidade do Porto, Rua Alfredo Allen, 208, 4200-135 Porto, Portugal

[e] Instituto de Ciências Biomédicas Abel Salazar, Universidade do Porto, Rua de Jorge Viterbo Ferreira, 228, 4050-313 Porto, Portugal

[f] Faculdade de Medicina, Universidade do Porto, Al. Prof. Hernâni Monteiro, 4200 - 319 Porto, Portugal

[g] Institut Pasteur, 25-28 Rue du Dr. Roux, 75015, Paris, France

[h] UCIBIO, REQUIMTE, Laboratory of Pharmaceutical Technology, Department of Drug Sciences, Faculty of Pharmacy, University of Porto, Rua de Jorge Viterbo Ferreira, 228, 4150-755 Porto, Portugal

* Corresponding author(s): i3S - Instituto de Investigação e Inovação em Saúde, Universidade do Porto, Rua Alfredo Allen, 208, 4200-135 Porto, Portugal. Tel.: +351 220408800; Email: icastro@ineb.up.pt (Inês C. Gonçalves)

Declarations of interest: none.

Abstract

Persistent *Helicobacter pylori* (*H. pylori*) infection is related to 90% of gastric cancers. With bacterial resistance rising and treatment inefficiency affecting 15% of the patients, alternative treatments urge. Chitosan microspheres (ChMics) have been proposed as an *H. pylori*-binding system. This work evaluates ChMics biocompatibility, mucopenetration and capacity to treat *H. pylori* infection in mice after oral administration. ChMics of different size (XL, ~120 µm and XS, ~40 µm) and degree of acetylation (6% and 16%) were developed and revealed to be able to adhere both human and mouse-adapted *H. pylori* strains without cytotoxicity towards human gastric cells. *Ex vivo* studies showed that smaller (XS) microspheres penetrate further within the gastric foveolae, suggesting their ability to reach deeply adherent bacteria. *In vivo* assays showed 88% reduction of infection when *H. pylori*-infected mice (C57BL/6) were treated with more mucoadhesive XL6 and XS6 ChMics. Overall, ChMics clearly demonstrate ability to reduce *H. pylori* gastric infection in mice, with chitosan degree of acetylation being a dominant factor over microspheres' size on *H. pylori* removal efficiency. These results evidence the strong potential of this strategy as an antibiotic-free approach to fight *H. pylori* infection, where microspheres are orally administered, bind *H. pylori* in the stomach and remove them through the gastrointestinal tract.

Keywords: microparticles, biomaterials, bacteria adhesion, mucoadhesion, *in vivo*

Statement of Significance

Approximately 90% of gastric cancers are caused by the carcinogenic agent *Helicobacter pylori*, which infects >50% of the world population. Bacterial resistance, reduced antibiotic bioavailability, and the intricate distribution of bacteria in mucus and within gastric foveolae hamper the success of most strategies to fight *H. pylori*. We demonstrate that an antibiotic-free solution based on bare chitosan microspheres to bind and remove *H. pylori* from stomach, can achieve 88% reduction of infection from *H. pylori*-infected mice. Changing size and mucoadhesive properties, microspheres can reach different areas of gastric mucosa: smaller and less mucoadhesive can penetrate deeper into the foveolae. This promising, simple and inexpensive strategy paves the way for a faster bench-to-bedside transition, therefore holding great potential for clinical application.

Introduction

Helicobacter pylori (*H. pylori)* are human pathogens that specifically colonize the gastric epithelium of more than half of the world's population [1-4]. Since at least 90% of gastric cancers are related with this bacterium [5], *H. pylori* gastritis was recently designated as an infectious disease with the recommendation of treatment of all infected subjects [6]. Its eradication has been associated with a decrease in incidence and development of gastric cancer [7-9], although only few studies involving human cohorts have been performed [8, 10].

Current antibiotic-based therapies have been improved by varying and increasing the number of concomitant drugs administered and prolonging the duration of the treatment [11], taking into account the geographical bacterial resistance to the different recommended antibiotics [5]. However, even when performing susceptibility testing [12], the reduced antibiotic bioavailability at the site of action, poor patient compliance and the increasing resistance of *H. pylori* to antibiotics in most parts of the world [13, 14] are strong evidence that new therapies must be developed. Overcoming the suboptimal eradication rates is crucial for the 42-105 million patients for whom the treatment is inefficient (6-15% failure rate) [5, 11].

Alternative therapies to overcome these challenges have been comprehensively explored [15-18]. Focus has been given to understanding bacterial infection mechanisms and interaction with the host [19, 20], identifying bacterial specific molecules that may represent potential targets, such as bacterial virulence factors, urease, flagella or surface adhesins [21-23]. The combination of these targets with improved encapsulation systems for local delivery of antibiotics (using micro- or nano- systems) [24-33], usage of compounds from natural sources [34-41] or vaccination [42-45] has allowed the development of more precise and efficient systems aiming *H. pylori* eradication.

Chitosan is a natural biocompatible [46] polysaccharide recurrently explored for gastric applications due to its mucoadhesive properties [47, 48] associated with the $-NH_2$ groups that become protonated at acidic pH, establishing electrostatic interactions with both the negatively charged gastric mucins at the acidic stomach pH and the bacterial membrane [49-51]. Moreover, chitosan has bactericidal properties against a wide range of bacteria [46, 52, 53], including *H. pylori* [54, 55].

Our group has previously shown that ChMics produced by ionotropic gelation with a diameter of around 170 µm and with chitosan degree of acetylation (DA) of 16% and crosslinked with genipin are stable in acidic conditions, and mucoadhesive with a mice gastric retention time of 2h [49]. Afterwards, we demonstrated that these ChMics are not cytotoxic and can adhere several strains of *H. pylori* under different pH [56]. Lastly, these ChMics were

modified with glycans to make them *H. pylori*-strain specific, being able to prevent/remove *H. pylori* adhesion to gastric mucosa expressing the same glycans (*in vitro* and *ex vivo*) [57]. These findings reveal the potential of these ChMics as an antibiotic-free alternative system to fight gastric infection.

As such, the aim of this work is to validate the use of ChMics as an orally administrated system to bind *H. pylori* in the stomach and remove them through the gastrointestinal tract of *H. pylori* infected mice. Knowing that *H. pylori* are present not only in the stomach mucus layer, but also within the gastric foveolae (gastric pits - depressions in gastric mucosa, 70 µm width), lining on and between the surface mucous cells covering the apical part of this structure [58], ChMics with two sizes were developed (~40 µm and ~120 µm). We hypothesize that smaller ChMics would be able to penetrate gastric foveolae. In addition, since the DA of chitosan can influence ChMics mucoadhesion, ChMics were prepared with chitosan with two different DA (6% and 16%). All ChMics were produced using an aerodynamically driven system envisaging a large-scale production. ChMics interaction both with bacteria and human gastric carcinoma cells were assessed, *ex vivo* studies to evaluate ChMics mucopenetration conducted, and ChMics efficiency to bind and remove of *H. pylori* from infected C57BL/6 mice explored.

Materials and Methods

Preparation of chitosan microspheres

Squid pen chitosan (Ch) powders (France Chitine) with degree of acetylation (DA) of 6% (Molecular weight, MW ~400 kDa; provided by the manufacturer) and 16% (MW ~324 kDa; determined by high-performance size-exclusion chromatography (HP-SEC) [59]) were purified as previously described by Amaral, I., *et al.* [60]. DA of purified Ch was confirmed as reported by us [59] using Fourier transform infrared spectroscopy (FT-IR) and based on the method proposed by Brugnerotto *et al*. (2001) [61], where the amide III band at 1320 cm^{-1} (C–N stretching vibration) was used as the analytical band and the band at 1420 cm^{-1} (in plane O–H deformation vibration) was used as internal reference band (Figure S1).

Ch microspheres (ChMics) were prepared from Ch solutions in 0.1 M acetic acid [49] using an aerodynamically assisted spraying system (Nisco Encapsulation Unit Var J30, NISCO). Briefly, Ch solution exits a pressurized chamber in a conical spray, due to a regulated compressed air beam, into a sodium triphosphate pentabasic (TPP; 5% w/v in ddH_2O; pH 9.0; Sigma-Aldrich) solution. Ionotropic gelation is the basic production process, although coacervation of the Ch chains also occurs. Different variables were tested (Figure S2), namely Ch solution concentration (0.5% and 1% w/v), air stream pressure (0.153 - 0.525 barg) and nozzle diameter (0.25 and 0.5 mm). Table 1 depicts the selected parameters for each variable to produce particles with size around 120 µm diameter (XL ChMics) and around 40 µm diameter (XS ChMics), for both 6% and 16% Ch DA. Larger ChMics produced with

Ch with DA 16% solution were named XL16, while the ones produced with Ch solution with DA 6% were named XL6. Similar nomenclature was given to the smaller particles, namely XS16 and XS6, respectively.

Table 1 - Selected parameters for XL16, XL6, XS16 and XS6 ChMics production in the aerodynamically driven system.

	Ch degree of acetylation	Ch solution concentration	Syringe pump flow rate	Air stream pressure	Nozzle diameter
XL16 ChMics	16%	1% w/v	3.6 mL/min	0.153 barg	0.5 mm
XL6 ChMics	6%	1% w/v	2.5 mL/min	0.205 barg	0.5 mm
XS16 ChMics	16%	1% w/v	2 mL/min	0.307 barg	0.5 mm
XS6 ChMics	6%	0.5% w/v	0.5 mL/min	0.525 barg	0.25 mm

After production, ChMics were rinsed thrice with type I water and incubated in a 10 mM genipin (Wako Chemicals GmbH) solution (in 0.01 M phosphate buffered saline (PBS), pH 7.4). The crosslinking level of ChMics was followed by fluorescence time-lapse over 3 h using an Inverted Fluorescence Microscope (IFM, AxioVert, Zeiss) (Figure S3). Particles used in subsequent studies were crosslinked for 45 min at 25 °C, under 120 rpm. After crosslinking, ChMics were rinsed thrice with type I water, frozen in liquid nitrogen and lyophilized. ChMics were either stored dry or dispersed in ethanol (70% v/v). After suspending the microspheres and/or homogenizing the dispersion, a known volume (20 µL) was transferred into a black 96-well plate, microspheres allowed to settle, and images of the whole well acquired with a high-content screening (HCS) microscope (IN Cell Analyzer 2000, GE Healthcare, Nikon 2x objective). Using the IN Cell Developer Toolbox (GE Healthcare) software, the stitching of all images from each well was performed. ChMics in each well (per 20 µL) were counted using ImageJ software and the number of microspheres per mL determined for use in further studies. ChMics behavior and stability under acidic conditions (Simulated Gastric Fluid, HCl 0.2 M and NaCl 0.2 M; pH 1.2) was confirmed (Figure S4).

ChMics characterization

ChMics size and morphology were determined by HCS microscopy and scanning electron microscopy (SEM). Pore size and interconnectivity were observed by transmission electron microscopy (TEM).

Size and morphology

ChMics morphological features were extracted using HCS microscopy (IN Cell Analyzer 2000, Nikon 10x/0.45 NA Plan Fluor objective). A small amount of a ChMics suspension in 70% v/v ethanol (around 25 µL) was transferred into a black 96-well plate (with clear polystyrene flat bottom) and bright field images of the particles obtained through a wide-field automated imaging system. A customized protocol was developed in the IN Cell Developer Toolbox software to allow particles' segmentation and individualization, in order to automatically extract their morphological features, such as circular diameter, maximum chord, area or form factor. Particles' form factor

and area were used as acceptance criteria. ChMics characteristics are shown as mean ± standard deviation and graphs can be automatically generated using the Spotfire™ DecisionSite™ software.

SEM allowed observation of the 3D structure and morphology of ChMics. Dry lyophilized ChMics were adhered onto carbon tape and coated with a thin layer of gold by sputtering to improve their conductivity. Observation was performed either using a Tabletop Microscope TM3030Plus, with different magnifications, observation modes (5 kV/ 15 kV/ EDX) and signaling detection (BSE – Backscattered electrons, SE – Secondary electrons, Mix), or a FEI Quanta 400FEG ESEM / EDAX Genesis X4M scanning electron microscope.

Pore size and interconnectivity

Lyophilized ChMics were evaluated by TEM using a JEOL JEM 1400 transmission electron microscope equipped with a CCD digital camera Orious 1100W. For that, ChMics were fixed with 1% paraformaldehyde (PFA, Merck) in phosphate buffer (PB; 0.1 M; pH 7.4) for 1 h, at 4 °C and rinsed twice with PB under 370 g for 10 min. Samples were afterwards dehydrated in ethanol solutions (70% v/v and 90% v/v) for 10 min each and twice in absolute ethanol (100%) for 10 min. ChMics were then embedded in LR White resin for 1 h at room temperature (RT) and included in a closed capsule with LR White at 40 °C for 24 h. The capsule was cut into ultra-thin sections (50-100 nm) using an ultramicrotome and sections were loaded into Nickel grids (with Formvar Carbon film).

H. pylori adhesion to ChMics

Two bacterial strains were selected for evaluation of ChMics ability to adhere *H. pylori*: a mouse-adapted *H. pylori* strain, SS1 [62], obtained from Institut Pasteur, France, and a human clinical isolate, J99 [63], obtained from Umeå University, Sweden.

H. pylori strains were grown on *H. pylori* solid medium composed of blood agar base 2 (Oxoid, Probiológica) plates supplemented with 10% defibrinated horse blood (Probiológica) and 0.2% of an antibiotic/antifungal cocktail with 6.25 g/L vancomycin (Sigma-Aldrich), 0.155 g/L polymixine B (Sigma-Aldrich), 1.25 g/L amphotericin B (Sigma-Aldrich) and 3.125 g/L trimethoprim (Sigma-Aldrich). Bacteria were incubated at 37 °C, for 48 h, under microaerophilic conditions and then spread and incubated for another 48 h. For use in subsequent adhesion studies, bacteria were harvested from the plates using 0.01 M PBS with Tween ® 20 (Sigma-Aldrich) (PBS-T), labelled with fluorescein isothiocyanate (FITC, Sigma-Aldrich; 0.1 mg/mL) and frozen as described elsewhere [64].

The adhesion assay was performed by incubating ChMics with FITC-labelled *H. pylori* strains at a final optical density (OD_{600}) of 0.04, corresponding to 1×10^7 colony forming units (CFU) per mL [65], for 2 h, at RT, under 90 rpm stirring in citrate-phosphate buffer at pH 6.0. After incubation, ChMics were rinsed five times by centrifugation (9000 g, 7 min) to remove non-adherent bacteria and gently transferred to microscope slides. A drop of fluorescence mounting medium (Vectashield, Vector Labs) was then added, and a glass coverslip placed on the top of the preparation. ChMics and adherent FITC-labelled *H. pylori* were visualized by confocal laser scanning

microscopy (CLSM, Leica SP5, Leica Microsystems) with excitation at 561 nm and 488 nm, respectively. For each microsphere, stacks from the whole microsphere were performed with a step size of 2.98 µm, and images were afterward superimposed using the Leica Application Suite Advanced Fluorescence (LAS AF) software.

ChMics cytotoxicity in vitro

ChMics cytotoxicity towards a human gastric adenocarcinoma cell line (AGS, ATCC® CRL-1739™) was evaluated using elution/extract and direct contact assays, according to the international standard ISO 10993-5;12 [66, 67].

AGS cells were grown in RPMI complete medium, consisting of RPMI 1640 medium with glutamax (Gibco, Invitrogen), supplemented with 10% inactivated (30 min, 56 °C) fetal bovine serum (FBS, Gibco), 10 U/mL penicillin (Biowest) and 10 µg/mL streptomycin (Biowest), at 37 °C in a humidified atmosphere of 5% CO_2. Cells were seeded either in 96-well TCPS plates (1×10^4 cells per well) or in 24-well TCPS plates (5×10^4 cells per well), for the extract method and the direct contact assay, respectively, under the same conditions mentioned above.

ChMics were sterilized in 70% v/v ethanol for 30 min and rinsed thrice through centrifugation (9000 g, 7 min) in medium before use.

Extracts assay

Liquid extracts of ChMics were prepared by incubation of ChMics in RPMI 1640 medium without supplementation (in a proportion of 4 cm^2 of materials per mL; 4 cm^2 correspond to 5000 XL ChMics and 50000 XS ChMics; 100% extract) for 24 h, 37 °C, at 150 rpm. The extraction vehicle (RPMI 1640 medium without supplementation) was subjected to the same extraction conditions and used as negative control whereas 1 mM hydrogen peroxide (H_2O_2) solution was used as a positive control of cytotoxicity. After 24 h, medium was supplemented with 10% inactivated FBS, 10 U/mL penicillin and 10 µg/mL streptomycin and filtered (0.22 µm).

Direct contact assay

For direct contact assay, different amounts of ChMics (500, 1000 and 2000 for XL ChMics and 1000, 10000 and 100000 for XS ChMics were suspended in fresh RPMI complete medium (800 µL). TCPS beads were used as negative control while 1 mM H_2O_2 was used as positive control of cytotoxicity.

After 24h of cell seeding, culture medium was replaced either by the liquid extracts (extract assay) or by the ChMics in fresh RPMI complete medium (direct contact assay). After 24 h incubation, the resazurin assay was performed to evaluate cell metabolic activity. For that, resazurin (20% v/v) was added to the wells and incubated for 4 h. Afterwards, 200 µL of supernatant was transferred to black 96-well plates and fluorescence measured (λ_{ex} = 530 nm, λ_{em} = 590 nm) in a microplate fluorometer (Spectra Max GeminiXS, Molecular Devices) [56]. Blanks for fluorescence emission subtraction were performed with complete culture medium, microspheres or TCPS

microspheres, all without cells. Cell viability was determined using the average of five or six replicates, being expressed as the percentage of the metabolic activity of treated cells in relation to cells in culture medium alone.

General cell morphology features were evaluated by cytochemistry. Briefly, cells were rinsed twice with PBS and fixed in 4% w/v PFA for 15 min. Cells were then rinsed with PBS and cell membrane permeabilized with 0.1% v/v Triton™ X-100 (Sigma-Aldrich) at 4 °C for 5 min. After rinsing with PBS, cells were incubated with phalloidin (Alexa Fluor 488, Molecular Probes) solution in PBS in a 1:100 dilution for 30 min in the dark. After a rinsing step with PBS, DAPI (Sigma-Aldrich) solution at 3 µg/mL was added to each well and incubated for 15 min in the dark. Finally, cells were rinsed and kept hydrated in PBS until observation by IFM (Carl Zeiss – Axiovert 200) using FITC (λ_{ex} / λ_{em} = 490/525 nm) and DAPI (λ_{ex} / λ_{em} = 350/470 nm) filters.

ChMics penetration into gastric mucus

C57BL/6 mice with 6 to 10 weeks, obtained from Animal House at i3S (Porto, Portugal), were euthanized by carbon dioxide inhalation. All animal procedures were approved by Direcção Geral de Alimentação e Veterinária (DGAV) and performed in compliance with the laws and institutional guidelines of the Ethical Committee of i3S and in accordance with the European Legislation on Animal Experimental through Directive 2010/63/EU. Humane endpoints were followed in accordance with the OECD Guidance Document on the Recognition, Assessment, and Use of Clinical Signs as Humane Endpoints for Experimental Animals Used in Safety Evaluation. Stomachs were excised, opened transversally and the food content gently removed using PBS, preserving the stomach mucus layer. Each half of the stomach was placed in a 6-well plate under humidified atmosphere to avoid tissue drying and used as an individual gastric mucosa sample.

The penetration assay was performed by adding ChMics in pH 6.0 (citrate-phosphate buffer solution) on top of the exposed mucosa followed by incubation for 2 h at 37 °C, stirring at 70 rpm. Samples were afterwards rinsed thrice by dipping the stomach in 1 mL of PBS to remove loosely adherent ChMics. ChMics penetration into the gastric mucus was assessed by HCS microscopy. Mice gastric mucosa was frozen in Optimum Cutting Temperature (OCT) medium and transversal cryosections of 50 µm from the whole stomach (total thickness of around 1.7 mm) were performed using a cryostat, transferred to microscope slides and stained with HCS CellMask™ Deep Red plasma membrane stain (1 µg/mL in PBS, ThermoFisher, Molecular Probes™) for 30 min at 37 °C without any fixation step. IN Cell Analyzer 2000 microscope was used to map and obtain the images of each slide. Acquisition was performed using a 10x objective lens in the brightfield and Cy3 channel to visualize ChMics and in the Cy5 channel to visualize gastric mucosa, with five z-stacks being taken for each slice, with a step size of 10 µm and 10% overlap for subsequent mosaic reconstruction using the IN Cell Developer Toolbox.

ChMics efficiency in vivo

H. pylori-infected C57BL/6 mice were used to evaluate the ability of ChMics to remove SS1 *H. pylori* strain.

C57BL/6 mice (5-6 weeks old, males, specific pathogen-free) were obtained from *Charles River Laboratories* (Massachusetts, USA). All animal procedures were performed in compliance with the laws and institutional guidelines of the Ethical Committee of i3S as previously described in *section 2.5*. Mice were housed inside ventilated cages in an Animal Biosafety level 2 (ABSL2) room of the animal facility, with a 12 h light/12 h dark cycle. Animals were fed with commercial pellet diets and sterile distilled water *ad libitum.* Enrichment material was used to guarantee animals' welfare, confirmed through observation of physical appearance and weight variations, registered weekly for each animal, until sacrifice.

H. pylori infection of C57BL/6 mice

24 h before infection mice were transferred to clean cages without corncob or food, but with proper enrichment material to guarantee animals' welfare, and fasted (water privation only 3 h before infection). Mice were infected by oral gavage with 0.2 mL of SS1 *H. pylori* strain suspension of 1×10^{10} CFU/mL in peptone water, twice with two days interval. Non-infected control mice (Hp-) were given the same volume of peptone water. Food/water access was re-established 2 h after infection.

ChMics treatment

Four weeks after infection, mice were divided into groups and the ChMics treatment plan applied during a 14 days period. Scheme 1 shows the study protocol applied, experimental parameters and the infected animals test groups. In non-infected control animals (Hp-) ChMics were administered following the same protocol, in order to evaluate biocompatibility of ChMics.

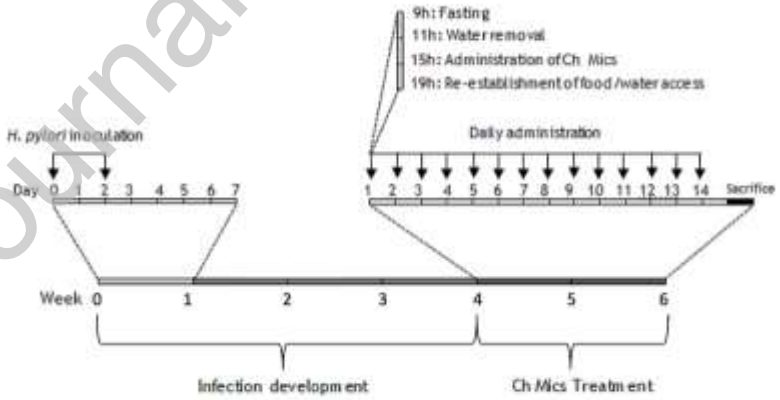

	Experimental setup 1	Experimental setup 2
Treatment duration	14 days	14 days
Number of administrations	1 administration/day	1 administration/day
Number of ChMics	1000 **XL16** ChMics 1000 **XL6** ChMics 100000 **XS16** ChMics	1000 **XL16** ChMics 1000 **XL6** ChMics 100000 **XS16** ChMics 100000 **XS6** ChMics

Administration vehicle	citrate-phosphate buffer pH6	citrate-phosphate buffer pH6
Volume of administration vehicle	0.2 mL	0.2 mL
Group name and number of animals per group (n)	Hp+ (12) Hp+XL16 (12) Hp+XL6 (12) Hp+XS16 (12)	Hp+ (9) Hp+XL16 (8) Hp+XL6 (8) Hp+XS16 (8) Hp+XS6 (8)

Scheme 1 – Study protocol and experimental conditions for the assessment of ChMics efficacy in the treatment of SS1 *H. pylori* infection in C57BL/6 mice. Groups: infected animals (Hp+), infected animals treated with XL16 ChMics (Hp+XL16), infected animals treated with XL6 ChMics (Hp+XL6), infected animals treated with XS16 ChMics (Hp+XS16), infected animals treated with XS6 ChMics (Hp+XS6).

Animals' sacrifice

At the end of the treatment plan, 24 h fasted mice were euthanized by cervical dislocation, with previous anesthesia (50-75 mg/kg ketamine and 0.5-1 mg/kg medetomidine) through intraperitoneal injection.

Mice stomachs were excised, opened transversally, rinsed in NaCl (to remove food contents) and cut accordingly to the Scheme 2. Briefly, each stomach was divided into 4 segments: two segments (parts A and B; half stomach) for *H. pylori* culture in blood agar plates (CFU) and Polymerase Chain Reaction (PCR) analysis, one segment for cryopreservation, and one segment for histological analysis. Similarly, two segments of mice liver from different lobes were collected for cryopreservation and histological analysis.

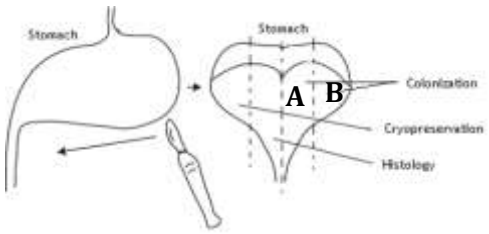

Scheme 2 - Schematic representation of the collection of mice stomach segments for analysis (cryopreservation, histological analysis and colonization).

Measurement of H. pylori gastric colonization

H. pylori infection levels in mice stomach tissue were quantified by colony forming assay. Each stomach portion (parts A and B) was collected to an Eppendorf ® tube with 400 µL of peptone water, weighed and homogenized with disposable sterile pistons. Dilutions of 10^1, 10^2 and 10^3 were made and spread with the correspondent non-diluted solution (10 µL of each solution) in *H. pylori* solid medium, prepared as previously described in section 2.3.,

supplemented with 50 mg/mL bacitracin (Sigma-Aldrich) and 20 mg/mL nalidixic acid (Sigma-Aldrich). After 15 days of culture at 37°C under microaerophilic atmosphere, colonies were counted and the number of colony forming units per mice stomach ($\mathrm{CFU/mice\ stomach} = (\mathrm{CFU/mL_{Part\ A}} + \mathrm{CFU/mL_{Part\ B}}) \times 2$) and per gram of stomach ($\mathrm{CFU/g} = \frac{\mathrm{CFU/mL\ Part\ A}}{\mathrm{m_{stomach\ Part\ A}}} + \frac{\mathrm{CFU/mL\ Part\ B}}{\mathrm{m_{stomach\ Part\ B}}}$) was calculated, where $m_{stomach}$ is the weight of the stomach segment.

PCR - Polymerase Chain Reaction analysis

Preparation of Genomic DNA for PCR assay

From the abovementioned 400 µL stomach homogenates, 100 µL were used for PCR analysis and genomic DNA isolation. Genomic DNA isolated by the salting out method from bacterial suspensions of SS1 *H. pylori* was used as positive control and of *Escherichia coli* DH5α as negative control [68]. Briefly, the stomach homogenates and the pellet of control bacteria (1×10^{10} CFU/mL) were incubated at 55 °C, for 2 h, on a thermal-shaker with 300 µL of lysis buffer [10 mM Tris (pH 7.5), 400 mM NaCl, 2 Mm EDTA (pH8)] (pH 7.3 - 7.5), 15 µL of 20% sodium dodecyl sulphate (SDS) and 10 µL of 20 mg/mL proteinase K. Afterwards, 100 µL of 100 M NaCl were added and samples were mixed and centrifuged at 17000 g for 15 min. The supernatant was transferred to a clean *Eppendorf* ® tube and 800 µL of 100% v/v ethanol were added to each sample, mixed and centrifuged at 17000 g for 5 min. DNA pellets were washed with 70% v/v ethanol, air dried and resuspended in 20 µL of sterile nuclease free-water.

The DNA concentration was measured using the NanoDrop ND-2000 spectrophotometer and the integrity of the genomic DNA was confirmed by 1.5% agarose gel electrophoresis.

Conventional PCR assay

PCR amplification of 26-kDa species-specific antigen (SSA) gene was performed using the primers SSAgeneF (5'-TGGCGTGTCTATTGACAGCGAGC-3') and SSAgeneR (5'-CCTGCTGGGCATACTTCACCAGTG-3'), 303 bp [69]. PCR was carried out in a 25 µL volume using 50 ng of genomic DNA, 10 µM of each primer, 25 mM $MgCl_2$, 10 mM dNTPs and 1 U of Taq DNA polymerase (ThermoScientific). PCR reactions were run in a thermal cycler (Applied Biosystems). The amplification protocol consisted on the initial denaturation at 95 °C for 4 min, 40 cycles of 30 sec at 95 °C, followed by 30 sec at 55 °C and 30 sec at 72 °C, plus a final extension of 8 min at 72 °C. A volume of 10 µL of each PCR product was analyzed by 1.5% agarose gel electrophoresis with ethidium bromide staining for the detection of amplified DNA.

Seven replicate experiments were performed using serial dilutions of 50, 5, 0.5, 0.05, 0.005, 0.0005, 0.00005 ng of template DNA of SS1 *H. pylori*. Negative (genomic DNA isolated from *Escherichia coli* DH5α) and positive (genomic DNA isolated from bacterial suspensions of SS1 *H. pylori*) control amplifications were performed in each experiment.

Histological analysis

Modified Giemsa staining was performed in microtome cut thin tissue sections (3 μm) of paraffin embedded stomachs to confirm bacterial infection. Samples were deparaffinated with xylene and rehydrated in ethanol (99.8%, 96% and 70% v/v ethanol), followed by a wash in running water. Samples were stained with 2% Giemsa solution for 30 min, washed in running water, dehydrated in ethanol (100% v/v ethanol) and diaphanized with xylene.

Hematoxylin and Eosin (H&E) staining was performed in paraffin embedded stomach and liver-tissues. Samples were deparaffinated and subsequently rehydrated as described above. Samples were then stained with Hematoxylin solution and rinsed with running water. After quick passages in ethanol solutions (70% and 96% v/v ethanol), samples were stained with Alcoholic Eosin solution, dehydrated with ethanol (99.8% v/v ethanol) and diaphanized with xylene.

After both staining, samples were mounted with entellan and observed under the optical microscope (Zeiss).

Statistical Analysis

Statistical analysis was performed using SPSS ® statistical software program (SPSS ® 24.0, Microsoft, USA). In the *in vitro* cellular experiments, Kruskal–Wallis was used to verify statistical significance between groups ($p < 0.05$). In the *in vivo* experiments, Mann-Whitney U-test was used to confirm that there were no significant differences between control groups (Hp+) of the two experimental setups ($p > 0.05$), allowing groups Hp+, Hp+XL16, Hp+XL6 and Hp+XS16 of experimental setups 1 and 2 to be analyzed together. Nonparametric Kruskal-Wallis was used to confirm statistically significant differences between groups ($p = 0.011$) and Mann-Whitney U-test with Bonferroni correction ($p < 0.0083$) was used to evaluate differences between these groups. Comparison between Hp+ and Hp+XS6 groups was performed using the Mann-Whitney U-test ($p < 0.05$), since Hp+XS6 group was only evaluated in experimental setup 2.

Results

ChMics characterization

The influence of microspheres size and chitosan degree of acetylation (DA) in the capacity of chitosan microspheres (ChMics) to bind and remove *H. pylori* from infected animals was explored by producing four types of ChMics with two sizes (120 μm and 40 μm) and two DA (6% and 16%), named as XL16, XL6, XS16, XS6 ChMics. The high voltage electrostatic system, previously used to produce microspheres with 170 μm diameter [49, 56, 57], allows only the production of particles with sizes between 100-350 μm, therefore not as small as desired. The

herein described aerodynamically driven system allows the production of a wider range of particle sizes (from 20 to 400 µm), being 75 times faster (mL/min comparing to mL/h), a relevant factor when envisaging a large-scale production. The thorough optimization process (data not shown) showed that particles size decreased with the increase of chitosan DA and air pressure and with the decrease of chitosan concentration and nozzle diameter (Figure S2).

Based on the genipin crosslinking kinetics of ChMics (Figure S3), 45 min was determined as the suitable crosslinking time to assure ChMics stability under acidic conditions while maintaining some protonated amines necessary for mucoadhesion and bacterial binding. These ChMics are stable and maintain their integrity and structure until at least 24h incubation at pH 1.2 (SGF, Figure S4), despite swelling and becoming more transparent with a gel-like structure.

A morphometric characterization of crosslinked and lyophilized ChMics was performed by HCS microscopy and SEM (Figure 1). XL and XS ChMics presented an average maximum chord (maximum center line through the target) of around 120 µm and 40 µm, respectively (Figure 1). According to the maximum chord values from Figure 1, the majority of the microspheres in each group (XL and XS ChMics) is in different ranges, despite there is a maximum overlap of ~25% between the smaller particles in the XL ChMics and the XS ChMics. Regarding morphology, XL and XS ChMics presented an irregular shape with an external porous structure and a rough surface, features caused mainly by the lyophilization process (intended to increase their shelf-life), with bigger particles presenting a more spherical shape (form factor (sphericity) = 0.9 ± 0.1 (circle = 1)) than smaller ones (form factor = 0.7 ± 0.1). SEM images show that independently of particles size, ChMics produced with chitosan DA of 16% present a surface with more micro-rugosities than the ones produced with chitosan DA of 6%, that have large and wide wrinkles. TEM images of ChMics sections revealed the presence of an internal pore interconnection (Figure S5), with XL16 ChMics presenting the biggest pore size (still below 5 µm), while XL6, XS16 and XS6 ChMics presented an overall pore size below 0.5 µm. However, images also suggest that there is no pore interconnection between the exterior of the ChMics and its internal porous structure.

XL16 ChMics **XL6 ChMics** **XS16 ChMics** **XS6 ChMics**

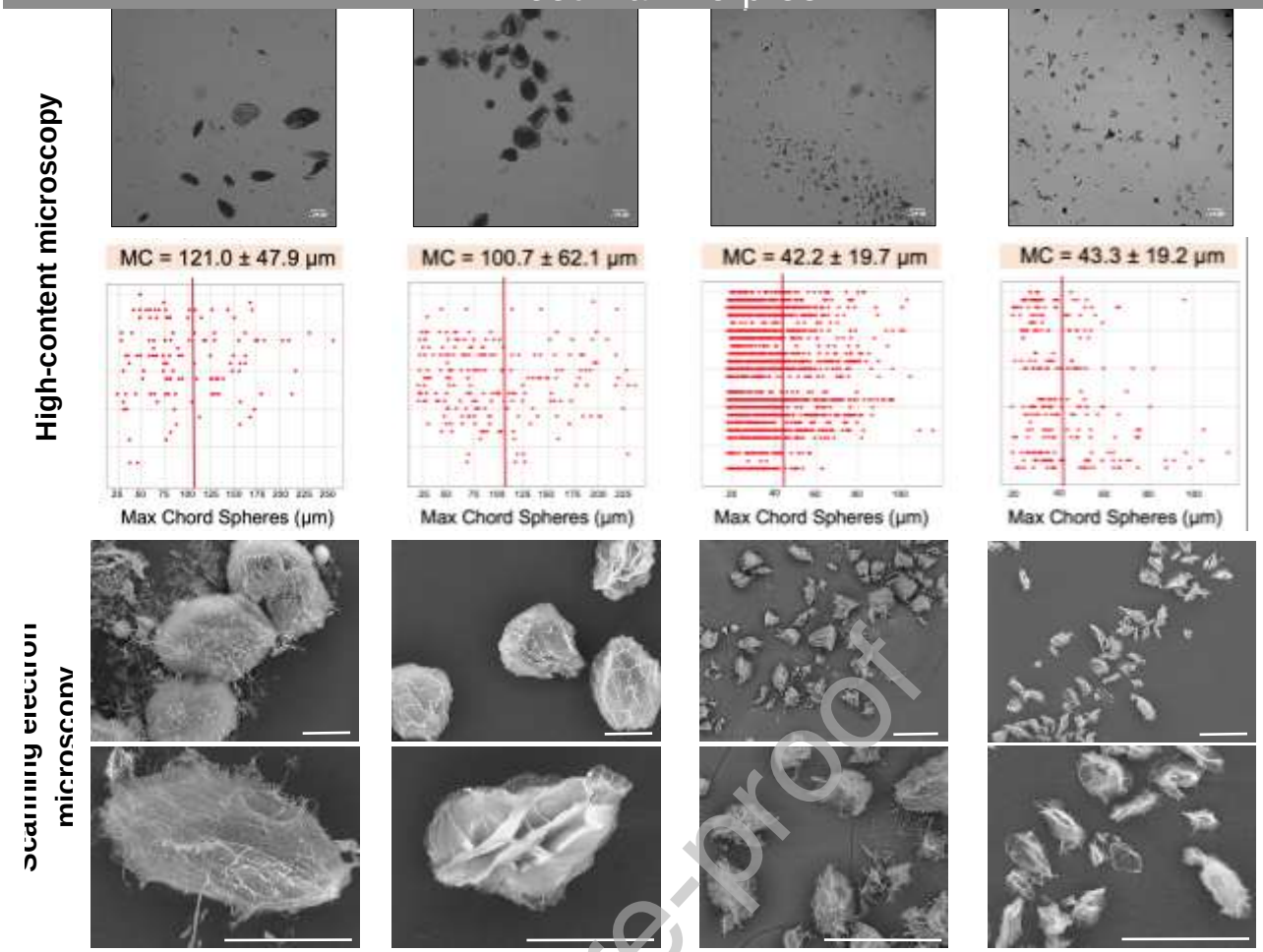

Figure 1 - ChMics size and morphology after lyophilization. On the top, images and graphs obtained by HCS microscopy and Spotfire™ DecisionSite™, respectively (MC = Maximum Chord). Scale bar = 100 µm. On the bottom, ChMics 3D structure and morphology obtained by SEM in two different magnifications. Scale bar = 100 µm.

H. pylori adhesion to ChMics

FITC-labelled mouse adapted SS1 *H. pylori* strain adhered to XL16, XL6, XS16 and XS6 ChMics (Figure 2), confirming their ability to bind bacteria through unspecific interactions, independently of chitosan DA and particles size. Adhesion of the human isolate *H. pylori* strain, J99, was also confirmed (Figure S6), widening the spectrum of action of these ChMics.

Quantification of bacterial adhesion to previously produced microspheres (~170 µm, DA of 16%) [56] was performed, showing around 100 adherent bacteria per microsphere (at pH 6.0). Based on this, it is expected that the herein presented XL ChMics (~120 µm) adhere around 70 bacteria/microsphere while the smaller ones (~40 µm) adhere around 23 bacteria/microsphere.

H. pylori adhesion to chitosan microspheres occurs independently of microspheres shape, as shown in our confocal microscopy images. Round shape is therefore not a requirement for our binding-strategy, despite the roughness (wrinkles and porosity) induced by lyophilization increases the surface area of contact with bacteria, therefore increasing the possibility of bacterial adhesion. Considering the lack of connection between the outside

surface and the internal porous structure (Figure S5) and according to the confocal microscopy z-stacks of the microspheres with adherent bacteria (data not shown), bacteria adhere mostly on the surface of the ChMics. *H. pylori* adhesion is not compromised by the crosslinking time of 45 min, suggesting the presence of protonated amine groups at the surface of the ChMics available for bacterial adhesion.

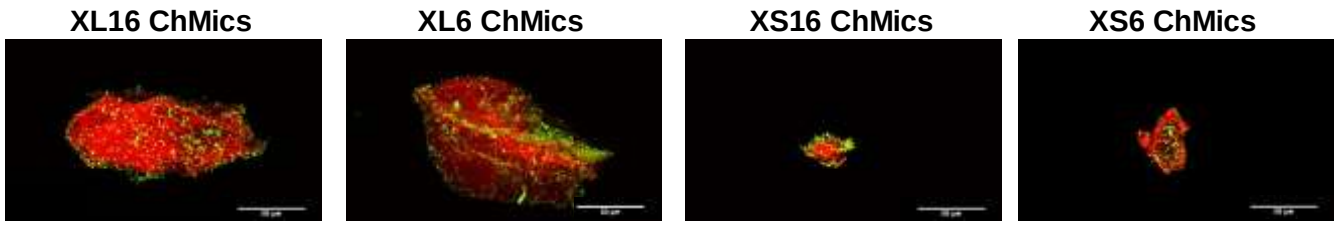

Figure 2 - FITC-labelled SS1 *H. pylori* adhesion to ChMics at pH 6.0. Images obtained by confocal microscopy with an excitation wavelength of 561 nm. ChMics in red with adherent bacteria in green. Scale bar = 50 µm.

ChMics in vitro cytotoxicity

Cytotoxicity was evaluated both through extract/elution method (Figure 3) and direct contact (Figure 4) test against a human gastric cell line, quantitatively by cell metabolic activity measurements and qualitatively through cytochemistry.

Experiments considering the liquid extracts of the microspheres were designed to assess the leaching of toxic products from the particles after incubation in an aqueous medium. Even though most of the particles should be removed from the gastrointestinal tract before chitosan starts degrading, interaction of the microspheres with gastric cells could still occur and/or particles can be retained in the mucus layer. Figure 3 shows that no reductions in the cell metabolic activity occurred when comparing each extract with the negative control (extraction medium), demonstrating that there is no leaching of toxic products from the particles.

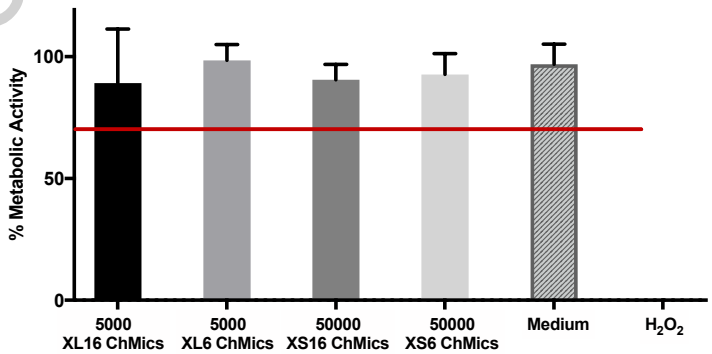

Figure 3 – Metabolic activity of AGS cells assessed by the extraction method. Resazurin assay was performed after 24 h incubation with liquid extracts of XL16, XL6, XS16 or XS6 ChMics, extraction medium (negative control) or 1 mM H_2O_2 (positive control). Metabolic activity is expressed as a percentage of the cell metabolic activity of treated cells in relation to cells in extraction culture medium only. ChMics amounts analyzed were in accordance with the international standard ISO 10993-12 [66],

following a proportion of 4 cm^2 of materials per mL: 4 cm^2 = 5000 XL ChMics and 50000 XS ChMics (100% extracts, non-diluted).

Similar results were obtained when cells were directly in contact with ChMics (Figure 4). Regarding XL16, XL6 and XS6 ChMics, a statistically significant decrease in cell metabolic activity was found when in the presence of the highest concentration evaluated (2000 for XL and 100000 for XS) (Figure 4.A). This can be associated with the high area of the well that is covered by ChMics, which may impair exchange of O_2, CO_2 and nutrients. However, and since according to the ISO standard only a reduction in cell viability of more than 30% is considered a cytotoxic effect, ChMics are considered cytocompatible in all concentrations tested, independently of the microspheres size and chitosan DA. As expected, in both tests, cells exposed to H_2O_2 showed extensive cell lysis and vacuolization, with less than 1% of the cells metabolically active.

ChMics cytocompatibility was also evaluated by cytochemistry, with gastric cells presenting a regular healthy morphology across conditions and comparing to the control, already forming in some cases a monolayer (Figure 4.B). Cells cultured in the presence of H_2O_2 died, and therefore detached from the bottom of plate, reason why no cells can be seen after staining.

Overall, no toxic effects were observed after 24 h incubation neither with the extracts nor in direct contact with the ChMics and therefore no effects are predictable for the approximately 2 h [49] that ChMics are expected to remain in the stomach.

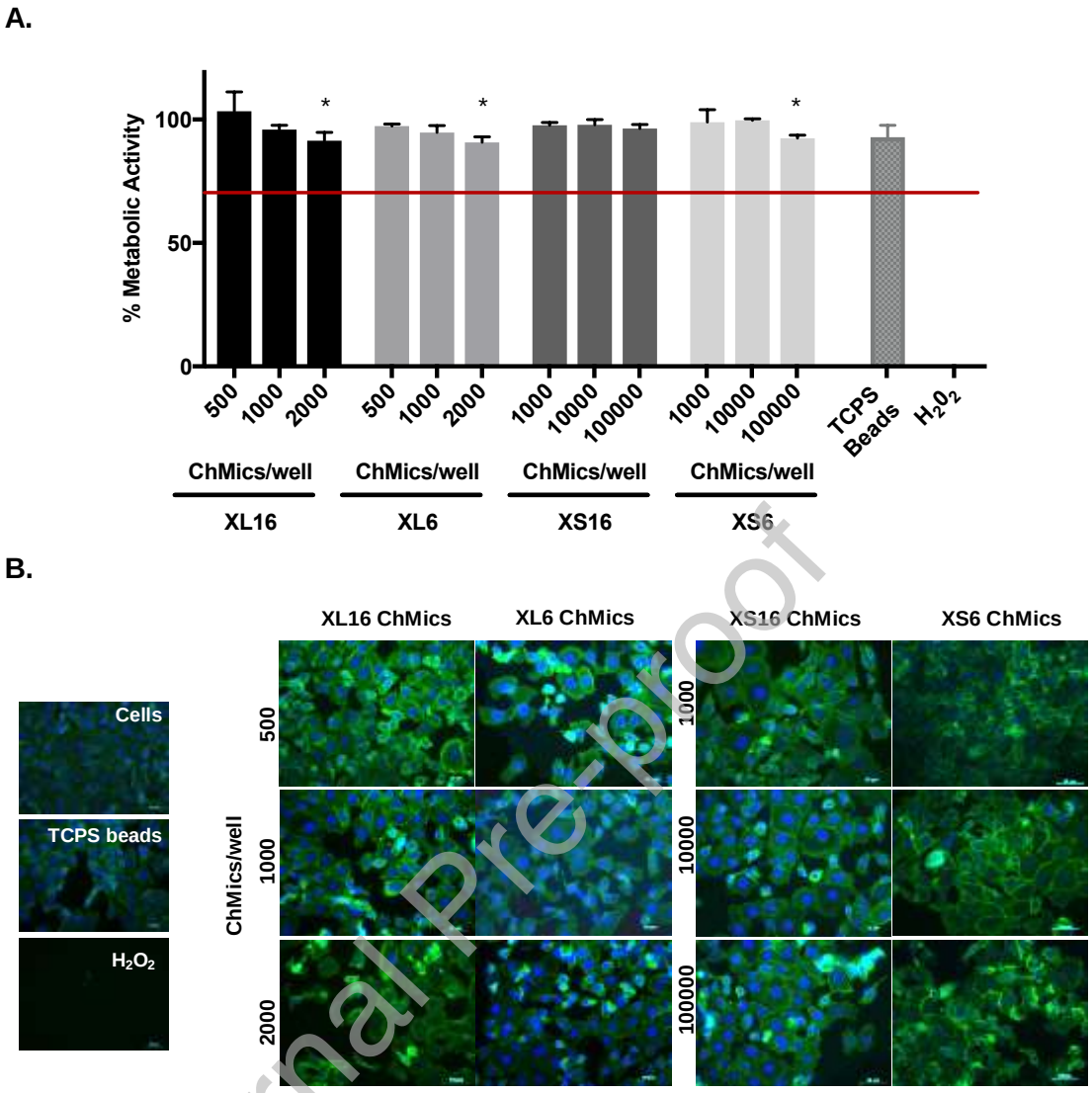

Figure 4 – Metabolic activity and morphology of AGS cells after direct contact with ChMics. **A.** Cell metabolic activity was assessed by the resazurin assay after 24 h incubation with ChMics (500, 1000 and 2000 for XL ChMics and 1000, 10000 and 100000 for XS ChMics), TCPS beads (negative control) or 1 mM H_2O_2 (positive control). Metabolic activity is expressed as a percentage of the cell metabolic activity of treated cells in relation to cells in culture medium only. *Samples significantly different from cells in culture medium only (Kruskal–Wallis, $p < 0.05$). **B.** Cells morphology was analyzed by cytochemistry: cells were stained with DAPI (nucleus) - blue and Phalloidin (F-actin in cytoskeleton) - green. Fluorescence images were taken by IFM after contact with ChMics. Scale bar = 50 µm.

ChMics penetration into the mucus layer

Ex vivo mice stomachs were used to infer om ChMics capacity to penetrate gastric mucosa since the *in vivo* evaluation was hampered by the similar fluorescence between ChMics and the stomach content, namely food and bedding material that persist even after 24 h fasting, making it impossible to clearly identify the ChMics.

Fluorescence labelling of the microspheres was not attempted [70, 71], since it would affect ChMics mucoadhesive properties (through reduction of the number of free amines).

Figure 5 illustrates different focal planes of mice gastric mucosa, from the superficial foveolar epithelium to the deeper areas, in a total thickness of ~1700 µm for each stomach. Due to its fast acquisition, HCS microscopy mapped the slices corresponding to the whole thickness of the stomach (Figure 5). Larger XL6 ChMics were mostly found in superficial focal planes (up to 350 µm depth), with a gradual decrease in particles number being observed until 450 µm, while smaller XS6 and XS16 ChMics were found in the superficial planes (up to 350 µm) but also deeper inside the stomach. More mucoadhesive XS6 ChMics were detected until a depth of ~1200 µm, with less mucoadhesive XS16 ChMics being found even deeper, at a depth of ~1500 µm.

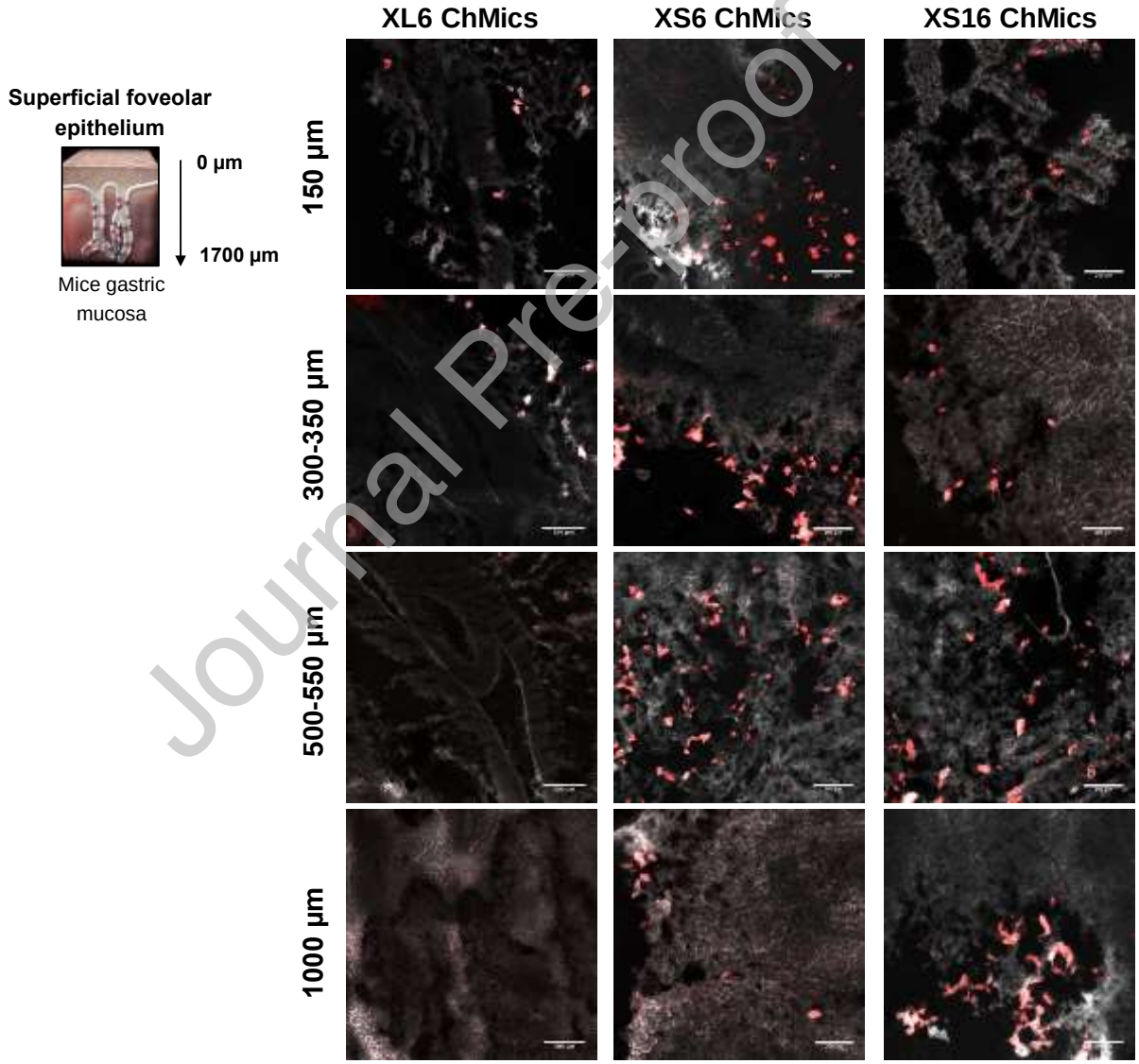

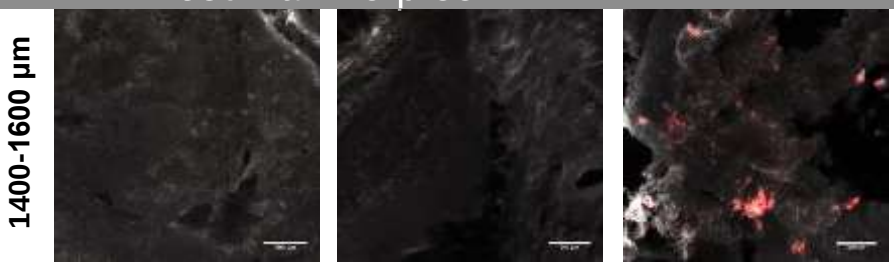

Figure 5 - Transversal cryosections of different depths of mice gastric mucosa (grey) with ChMics (red) adhered. Images were acquired by IN Cell Analyzer 2000 after labelling gastric mucosa with HCS CellMask™ Deep Red stain. ChMics can be observed in different depths of the gastric mucosa (rows) from the superficial foveolar epithelium to deeper areas. Scale bar = 500 µm (XL6 ChMics) and 200 µm (XS6 and XS16 ChMics).

ChMics efficiency in vivo

After confirming the capacity of ChMics to bind SS1 *H. pylori* strain, *in vitro* biocompatibility and mucopenetration ability, these particles were administered to C57BL/6 mice to evaluate their *in vivo* biocompatibility and efficiency in the treatment of *H. pylori* infection.

Infection of C57BL/6 mice with SS1 *H. pylori* strain was confirmed by CFU counting, PCR analysis, Modified Giemsa and Hematoxylin and Eosin (H&E) stains (Figure 6). Regarding CFU counting (Figure 6.A), average values of infection in *H. pylori*-infected animals (Hp+) were of 7×10^5 CFU/mice stomach, which corresponds to 10^7 CFU/g of stomach tissue. These values were found similar to the levels reported in literature, which for this SS1 strain has been around 10^5 to 10^8 CFU/g of stomach tissue of *H. pylori* approximately one month after infection [62, 72-77]. In control non-infected animals (Hp-), no *H. pylori* growth was verified, as expected. Highly sensitive PCR technique confirmed infection after bacterial DNA isolation from gastric tissue and amplification of SS1 *H. pylori* specific gene (Figure 6.B). The agarose gel showed successful amplification of 303 base pair product of 26-kDa gene SSA, reported as the most appropriate for *H. pylori* detection [78], in Hp+ animals. This fragment was clearly detectable in the progressive dilutions from SS1 *H. pylori* strain used as positive control. Modified Giemsa stain identified *H. pylori* on the surface of the gastric mucosa and in the mucus layer, confirming once again that the SS1 strain was able to effectively infect mice (Figure 6.C). H&E staining revealed differences in gastric mucosa morphology and structure between Hp- and Hp+ animals, with Hp+ animals presenting a more disorganized epithelium with a slight atrophy of the distal portion of this organ and revealing the presence of some mononuclear inflammatory infiltrates (Figure 6.D).

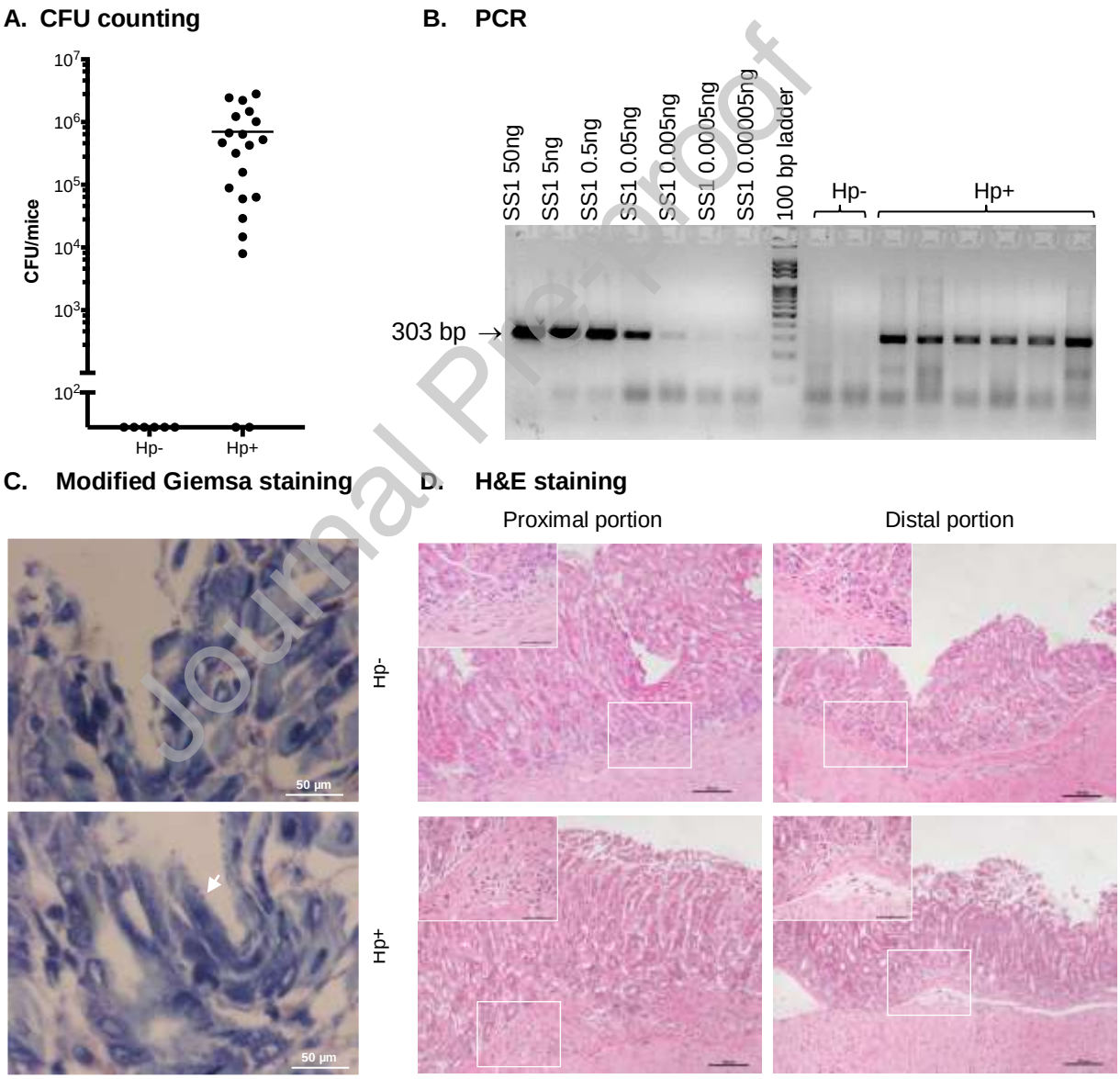

Figure 6 – Confirmation of C57BL/6 mice infection with SS1 *H.* pylori strain. **A.** CFU counting (CFU/mice stomach, number of bacteria colonies per mice stomach). **B.** PCR analysis (PCR amplifications of SS1 gene, from progressive dilutions of SS1 strain; arrow (303 bp) indicates the expected size of the SS1 *H. pylori* strain PCR products, validated by the third band of the 100 bp ladder – 300 bp). **C.** Modified Giemsa stain (scale bar = 50 µm; arrow reveals the presence of bacteria). **D.** H&E stain

(proximal and distal portion of glandular stomach, scale bar = 100 µm, inserts 50 µm). Hp-: non-infected animals, Hp+: infected animals.

Concerning ChMics efficiency in removing bacteria from infected mice stomach (Figure 7), statistically significant differences were found between Hp+ (average of 6.99×10^5 CFU/mice) and Hp+XL6 (average of 8.71×10^4 CFU/mice, $p = 0.002$) and Hp+ and Hp+XS6 groups (average of 8.11×10^4 CFU/mice, $p = 0.036$), with infection levels being reduced in 88% when animals were treated with either XL6 or XS6 ChMics. The decrease in Hp+XS16 treated group was very close to significance (average of 1.25×10^5 CFU/mice, $p = 0.018$), with infection levels reaching 82% reduction when treatment relied on XS16 ChMics.

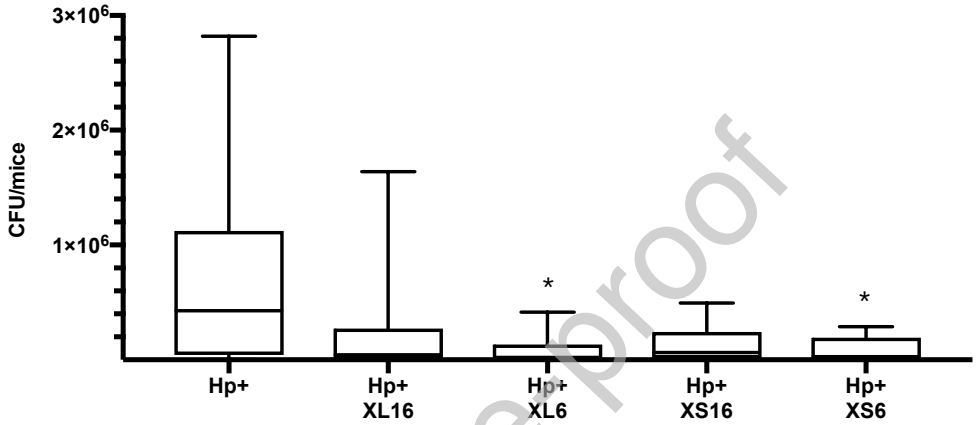

Figure 7 - Efficacy of treatment against *H. pylori* infection revealed by the presence of SS1 *H. pylori* strain in C57BL/6 mice stomach (CFU/mice stomach). Groups legend: infected but untreated mice (Hp+); infected and treated with XL16, XL6, XS16 and XS6 ChMics (Hp+XL16, Hp+XL6, Hp+XS16 and Hp+XS6, respectively). * Statistically significant differences from Hp+ group (Mann-Whitney U-test; $p < 0.0083$ for Hp+XL16, Hp+XL6 and Hp+XS16 and $p < 0.05$ for Hp+XS6).

Despite the repeated oral gavages and handling of animals throughout the two weeks of ChMics administration (week 4 to week 6), animals maintained their good physical appearance (normal fur, well groomed, alert and active) and body weight (Figure S7).

Assessment of ChMics *in vivo* toxicity was conducted through gastric and liver histopathology (H&E staining, Figure 8). Non-infected animals (Hp-, Hp-XL16, Hp-XL6, Hp-XS16, Hp-XS6 - first row) presented normal gastric architecture, with an organized structure and a well-defined gastric epithelium, even when ChMics were administered. There can be denoted, though, the presence of some minor inflammatory infiltrates in these groups, which is considered as a normal occurrence, if in a small extent [79]. In what concerns infected and treated animals (Hp+XL16, Hp+XL6, Hp+XS16, Hp+XS6), mononuclear inflammatory infiltrates can be found in a higher extent (although not in a quantitative way), as well as some mastocytes, both signs of chronic inflammation. However, the presence of ChMics does not seem to neither improve nor harm the gastric mucosa, since similar inflammatory infiltrates and cells were found across the different infected and treated animals. In fact, in a *H. felis* infected mouse model, more prone to develop robust inflammatory response and ultimately gastric adenocarcinoma, signs as

inflammation, metaplasia and dysplasia were found reversible with early eradication therapy, even after long-term infection [80].

Histological analysis of the liver of all groups of animals revealed a normal architecture of the tissue [81, 82], therefore demonstrating lack of side effects of ChMics. A radial distribution of hepatocytes around veins/arteries was observed with the associated bile ducts and some accumulation of hepatic fat (steatosis) in some animals, a normal result given the diet rich in carbohydrates that animals are subjected to in the animal facility (Figure 8).

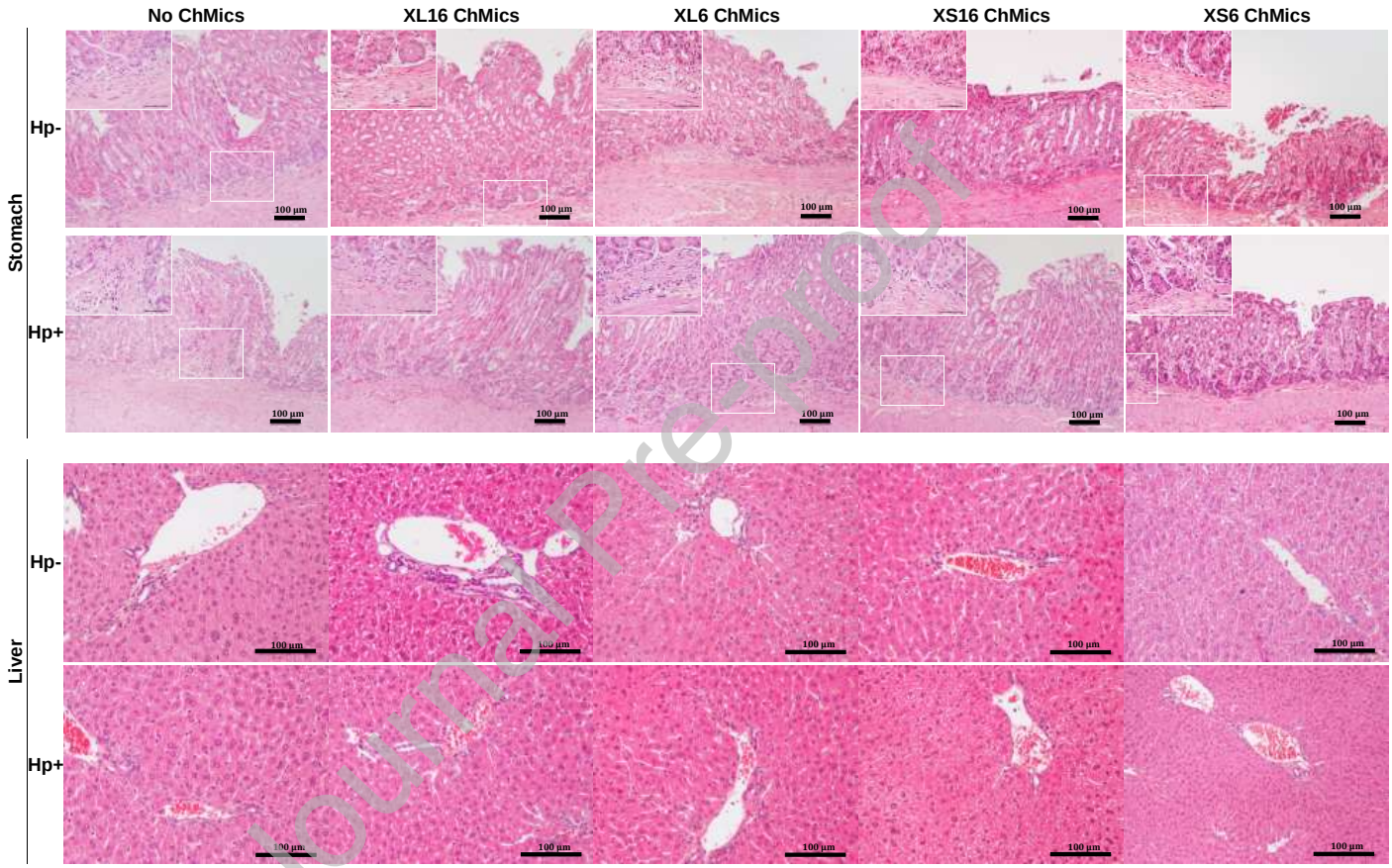

Figure 8 – Gastric and hepatic histological characterization (H&E staining) of non-infected (Hp-) and *H. pylori* infected (Hp+) C57BL/6 mice, afterwards treated with different ChMics (XL16, XL6, XS16 or XS6). Scale bar = 100 µm (inserts 50 µm).

Discussion

Improvement of the therapeutic strategies against *Helicobacter pylori* (*H. pylori)* infection has been a major challenge. Our antibiotic-free strategy validates the use of ChMics as an orally administrated system to bind *H. pylori* in the stomach and remove them through the gastrointestinal tract from *H. pylori* infected mice. The main goal of the work was to understand the impact of varying and combining parameters as size (XL, ~120 µm and XS, ~40 µm) and degree of acetylation (DA, 6% and 16%) on the microspheres capacity to penetrate gastric mucosa, and consequently on their ability to bind and remove bacteria therein present.

ChMics mucoadhesive properties and *H. pylori*-binding ability are dependent on the primary amines available in the chitosan chain. We had previously demonstrated that chitosan microspheres with DA 16% (170 µm) and 1h genipin crosslinking are stable over a range of pH (1.2, 2.6, 4.0, 6.0, and 7.4) [56] while maintaining their mucoadhesion to free mucins (Fernandes et al. 2013). As such, we herein controlled the crosslinking process through time-lapse fluorescence microscopy (Figure S3), and selected incomplete genipin crosslinking (45 min) to use in these studies. This allowed to maintain available some protonated amines necessary for mucoadhesion and bacterial binding, while at the same time assuring microspheres stability under harsh acidic conditions (pH 1.2). These ChMics are pH-responsive, swelling and becoming more transparent with a gel-like structure at lower pH, associated with protonation of chitosan NH_3^+ groups, despite maintaining their integrity and structure. Mi *et al.* [83] studied the effect of pH in TPP/genipin co-crosslinking of chitosan particles, showing that when particles are produced in high pH (pH 7.0 and 9.0), a slow ionic crosslinking and fast deprotonation of NH_3^+ groups of chitosan occurs, leading to a dominant chemical genipin crosslinking [83]. Although our reaction was performed in two steps (TPP followed by genipin), the TPP solution was at pH 9.0 and therefore we expect our particles to have high amounts of free amines available for the genipin crosslinking. Besides, since we use 10 times lower concentration of genipin and a reduced period of time (45 min *vs* 24 h), we do not have a complete reaction.

ChMics bind different *H. pylori* strains, including human isolates and SS1 mouse adapted strain, in an unspecific manner and independently of ChMics different size and DA. In previous

studies we had shown that chitosan microspheres also adhere other human strains [56]. This widens the applicability of the strategy, allowing it to be more safely and quickly implemented even without the need for susceptibility testing and knowledge on the infecting *H. pylori* strain. Specifically, it also confirmed the possibility of using an *in vivo* mouse model to test this strategy.

Ex vivo studies showed that the particles were able to adhere to the mucus layer and reach different locations of the stomach, with larger ChMics (XL) remaining in the upper plans of the gastric mucosa while smaller particles (XS) reached deeper inside, stressing out the influence of size on their penetration ability. Other studies have supported this, as Takeuchi, H. *et al.* [84] showed that smaller liposomes (339.2 nm) penetrate in a higher extent than larger ones (4.6 μm). In fact, particles larger than the mesh pore size can be trapped in the entanglement of the mucin fibers that sterically block or difficult their penetration through the mesh spacing [85, 86]. Despite having an increased size, particles with adequate coating (such as polymers with high hydrophilicity, neutral charge and low molecular weight) can also penetrate physiological human mucus [87]. In addition, higher DA associated with low mucoadhesivity can allow particles to penetrate further (less cationic amines to establish electrostatic and hydrophobic interactions with mucins densely coated with negative charges [85, 88]). This was corroborated by Arora, S. *et al.* [89], that demonstrated that less mucoadhesive nanoparticles infiltrate faster and penetrate deeper into the mucosal layers near the gastric epithelial cells of antrum region with time [89]. Sadio *et al.* [90] reported that smaller chitosan nanoparticles with lower mucoadhesivity (due to low charge density) have higher capacity of reaching further down into the mucus layers. Size and mucoadhesivity also have an impact on particles residence time in the stomach [86, 91]. Large chitosan-coated beads (600-1250 μm) have remained in Wistar rats stomach for at least 7 h (>85%) [27], while smaller liposomes (100 nm) until after 24 h [71]. Our previously produced chitosan microspheres with DA 16% (170 μm) remained in mice stomach for at least 2 h, with only less than 10% still present after 4 h [49, 56]. Therefore, the herein presented ChMics should be retained for at least 2 h.

Although *ex vivo* assays demonstrate that small microspheres (XS ChMics) penetrate further into the gastric mucosa, *in vivo* results showed that chitosan DA has more effect than size on the reduction of *H. pylori* load in the stomach of infected mice. In fact, although there are no

statistically significant differences between animal groups, both ChMics with the lower DA (Hp+XL6 and HP+XS6) present significant reduction of 88% *H. pylori* when comparing with untreated animals (Hp+). These results suggest that ChMics with lower DA remain longer in the mucus layer, increasing the overall interaction with bacteria. The presence of higher amounts of protonated amines on XL6 and XS6 ChMics can also be associated with higher antimicrobial effectiveness [92], allowing increased interaction with the negatively charged membrane of bacteria, as previously demonstrated in a range of pH (2.6, 4 and 6) [55].

Considering that in *our H. pylori* infection model the number of SS1 *H. pylori* found to colonize the C57BL/6 mice stomach is ~7.0×10^5 CFU/mice, and that each XL ChMics should adhere ~70 bacteria and each XS ChMics should adhere ~23 bacteria, around 10 000 XL ChMics and 30 000 XS ChMics would be necessary throughout the whole treatment. Since our administration scheme is performed over 14 days, at least 714 XL ChMics and 2 143 XS ChMics would have to be administrated each day. As such, we assumed that 1 000 XL and 10 000 XS ChMics would be sufficient to remove all bacteria form the stomach. However, the pilot study performed with 10 000 XS6 ChMics showed no significant reduction when comparing to non-treated mice. Since both *in vitro* and *in vivo* cytotoxicity studies revealed the safety of using 100 000 XS ChMics subsequent studies were performed with this amount. Still, full eradication of *H. pylori* from the mice stomach was not achieved for all animals after ChMics administration.

Chitosan's protonated amine groups at acidic pH confer ChMics positive charge, allowing them to bind bacteria and adhere to the mucus layer, both negatively charged. Having seen that ChMics bind *H. pylori* independently of size and degree of acetylation, and adhere/penetrate the gastric mucosa (smaller ChMics penetrate deeper), we suggest as mechanism of action that upon oral administration, mucoadhesive ChMics bind *H. pylori* in the stomach and remove them through the gastrointestinal tract. ChMics with lower chitosan DA (6%) are more efficient in reducing *H. pylori* load in the stomach of infected mice. We hypothesize that due to higher mucoadhesion, these ChMics (XL6 and XS6) remain longer in contact with the gastric mucosa, increasing the possibility of interaction with bacteria. Ultimately, the clearance of the ChMics from the stomach is dependent on the physiological turnover time of the mucus layer, and therefore should take between 4 to 6 h [85]. This has been verified by us using similar microspheres (DA16%; 170 µm) [49], with the majority of ChMics already in distal part of the

intestine after 4h. Continuous and rapid secretion of gastric mucus and clearance efficiently removes pathogens and orally administered particles that fail to penetrate the loosely adherent layer of GI mucus and reach the firmly adherent layer [86, 93]. Particles must penetrate mucus at rates markedly faster than mucus renewal and clearance (turnover time is different according to the location in the gastrointestinal tract) in order to overcome the barrier [85].

Despite the promising 88% bacterial reduction, eliminating around 9 million bacteria (1 log reduction), there are still 1 million bacteria that remain in the stomach. Comparing to other studies with similar infection values (10^6 – 10^8 CFU/g stomach [74-76]), this study presents lower log reductions. However, we allowed the infection to be established for 1 month instead one or two weeks before performing the treatment. Nevertheless, ChMics ability to reduce *H. pylori* presence in the stomach could be potentially improved through exploitation of several approaches. Specifically regarding the treatment duration, for instance, although the 2 weeks treatment applied followed the guidelines of the currently used antibiotic therapy [5] aiming to cope with patient compliance, an increase in the period of treatment as used in some works (up to 4 [94] and 10 weeks [27]) could potentiate the effects of the ChMics. Enhancing the specificity of ChMics for *H. pylori* through immobilization of bacteria specific ligands on the ChMics surface, such as carbohydrates and other targetable molecules, has also been explored. Lewis b and sialyl-Lewis x-coated chitosan microspheres revealed an increased ability to target and remove *H. pylori* from mice stomachs (*ex vivo*) in comparison with bare ChMics [57]. High specificity and *in vivo* anti-*H. pylori* efficiency was observed when urea or fucose were incorporated in nanoparticles [30, 32], as reported for pH-sensitive amoxicillin-loaded ureido-conjugated chitosan derivatives (UCCs)-conjugated poly(lactic-co-glycolic acid) nanoparticles (AMX-PLGA/UCCs-2) [30] or berberine-loaded fucose-conjugated nanoparticles [32]. Aiming to compete with the epithelial cells for the binding of *H. pylori*, these strategies show improved antibacterial action towards *H. pylori* when compared to the systems without immobilized molecules or to antibiotics alone. Linoleic acid incorporated in a liposomal formulation (LipoLLA) has also shown a significant reduction of *H. pylori* load in C57BL/6 mice by ~2.5 orders of magnitude compared with infected non-treated animals [71].

The herein proposed strategy should primarily be seen as an antibiotic-free approach. Avoidance of antibiotics is advantageous in a long-term scenario, particularly considering the

side effects associated with the antibiotic-based eradication therapy against *H. pylori,* such as alteration of gut microbiota in terms of richness, diversity, and composition [5, 95] and the appearance of antibiotic-resistant components of gut microbiota [96]. However, ChMics can also be envisaged for administration in combination with antibiotics, potentially improving the efficacy of the existing antibiotics and providing a solution for the 42-105 million patients for whom the current antibiotic based-therapy is inefficient [5, 11]. Preferentially, ChMics concomitant administration with other natural compounds, reported to have interesting effects on *H. pylori* but without 100% efficacy, could also improve the overall efficacy of our strategy. Docosahexaenoic acid (DHA) revealed antibacterial action towards *H. pylori*, both *in vitro* and *in vivo*, in a dose-dependent manner, also decreasing mouse gastric mucosa inflammation [77]. This effect was further enhanced when encapsulating DHA in a delivery system, inhibiting *H. pylori in vitro* growth at lower concentrations (25 μM) than free DHA (>100 μM) [36].

Future work could include the deep exploitation of different combinations of microspheres and different treatment schemes, namely regarding amounts of microspheres, total treatment duration and number of administrations, vehicle of administration, need of fasting, among others. Even though the results obtained using this mouse model cannot be directly extrapolated to humans, our findings allow to conclude that these non-cytotoxic mucoadhesive ChMics are able to remove bacteria from infected mice stomach. As such, these ChMics can be interesting for human testing, revealing potential as an antibiotic-free alternative treatment to gastric infection.

Conclusions

In summary, we evaluated the *in vivo* efficiency removal of *H. pylori* from mice gastric mucosa after oral administration of large (XL, ~120 μm) and small (XS, ~40 μm) ChMics prepared using chitosan with different DA (6% and 16%). All partially crosslinked ChMics were stable in acidic conditions and able to adhere different *H. pylori* strains *in vitro* without causing cytotoxicity towards human gastric cells. Although smaller and less mucoadhesive (XS16) ChMics presented improved ability to penetrate further into the gastric foveolae, *in vivo* results showed a significant reduction of 88% in levels of infection when more mucoadhesive XL6 and

XS6 ChMics were used to treat SS1 *H. pylori*-infected C57BL/6 mice. The DA seems therefore to be a prevalent factor over size regarding ChMics efficiency to fight *H. pylori* gastric infection in mice. Overall, these results indicate this strategy as an effective and safe antibiotic-free approach to treat *H. pylori* infection.

Acknowledgments

This work was financed by PTDC/CTM-BIO/4043/2014 and by Portuguese funds FCT UID/BIM/04293/2019, EXPL/CTM-BIO/0762/2013 and by L'Oreal Portugal/FCT/UNESCO. Authors wish to thank FCT for Inês C. Gonçalves research position (IF/01479/2015), Catarina L. Seabra PhD grant (SFRH/BD/89001/2012) and Patrícia C. Henriques PhD grant (SFRH/BD/120154/2016).

The authors acknowledge the support of the Bioimaging Center for Biomaterials and Regenerative Therapies (b.IMAGE), member of the PPBI (PPBI-POCI-01-0145-FEDER-022122), for the imaging data acquisition using equipment maintained by the center, the support of the BioSciences Screening i3S Scientific Platform, CCGEN and Paula Magalhães for the help during the PCR analysis.

Declaration of interests

The authors declare that they have no known competing financial interests or personal relationships that could have appeared to influence the work reported in this paper.

References

[1] D.B. Polk, R.M. Peek, Jr., Helicobacter pylori: gastric cancer and beyond, Nature Reviews Cancer 10(6) (2010) 403-14.
[2] J.K.Y. Hooi, W.Y. Lai, W.K. Ng, M.M.Y. Suen, F.E. Underwood, D. Tanyingoh, P. Malfertheiner, D.Y. Graham, V.W.S. Wong, J.C.Y. Wu, F.K.L. Chan, J.J.Y. Sung, G.G. Kaplan, S.C. Ng, Global Prevalence of Helicobacter pylori Infection: Systematic Review and Meta-Analysis, Gastroenterology 153(2) (2017) 420-429.
[3] K. Kotilea, P. Bontems, E. Touati, Epidemiology, Diagnosis and Risk Factors of Helicobacter pylori Infection, in: S. Kamiya, S. Backert (Eds.), Helicobacter pylori in

Human Diseases: Advances in Microbiology, Infectious Diseases and Public Health Volume 11, Springer International Publishing, Cham, 2019, pp. 17-33.
[4] M. Leja, I. Grinberga-Derica, C. Bilgilier, C. Steininger, Review: Epidemiology of Helicobacter pylori infection, Helicobacter 24 Suppl 1 (2019) e12635.
[5] P. Malfertheiner, F. Megraud, C.A. O'Morain, J.P. Gisbert, E.J. Kuipers, A.T. Axon, F. Bazzoli, A. Gasbarrini, J. Atherton, D.Y. Graham, R. Hunt, P. Moayyedi, T. Rokkas, M. Rugge, M. Selgrad, S. Suerbaum, K. Sugano, E.M. El-Omar, H. European, G. Microbiota Study, p. Consensus, Management of Helicobacter pylori infection-the Maastricht V/Florence Consensus Report, Gut 66(1) (2017) 6-30.
[6] K. Sugano, J. Tack, E.J. Kuipers, D.Y. Graham, E.M. El-Omar, S. Miura, K. Haruma, M. Asaka, N. Uemura, P. Malfertheiner, C. faculty members of Kyoto Global Consensus, Kyoto global consensus report on Helicobacter pylori gastritis, Gut 64(9) (2015) 1353-67.
[7] K. Fukase, M. Kato, S. Kikuchi, K. Inoue, N. Uemura, S. Okamoto, S. Terao, K. Amagai, S. Hayashi, M. Asaka, Effect of eradication of Helicobacter pylori on incidence of metachronous gastric carcinoma after endoscopic resection of early gastric cancer: an open-label, randomised controlled trial, The Lancet 372(9636) (2008) 392-397.
[8] Y.C. Lee, T.H. Chen, H.M. Chiu, C.T. Shun, H. Chiang, T.Y. Liu, M.S. Wu, J.T. Lin, The benefit of mass eradication of Helicobacter pylori infection: a community-based study of gastric cancer prevention, Gut 62(5) (2013) 676-82.
[9] A.C. Ford, D. Forman, R.H. Hunt, Y. Yuan, P. Moayyedi, Helicobacter pylori eradication therapy to prevent gastric cancer in healthy asymptomatic infected individuals: systematic review and meta-analysis of randomised controlled trials, BMJ 348 (2014) g3174.
[10] B.C. Wong, S.K. Lam, W.M. Wong, J.S. Chen, T.T. Zheng, R.E. Feng, K.C. Lai, W.H.C. Hu, S.T. Yuen, S.Y. Leung, D.Y.T. Fong, J. Ho, C.K. Ching, J.S. Chen, Helicobacter pylori Eradication to Prevent Gastric Cancer in a High-Risk Region of China. A Randomized Controlled Trial, The Journal of the American Medical Association 291 (2004) 187-194.
[11] H. Jaka, A. Mueller, C. Kasang, S.E. Mshana, Predictors of triple therapy treatment failure among H. pylori infected patients attending at a tertiary hospital in Northwest Tanzania: a prospective study, Bmc Infect Dis 19 (2019).
[12] A. O'Connor, J.P. Gisbert, C. O'Morain, S. Ladas, Treatment of Helicobacter pylori Infection 2015, Helicobacter 20 Suppl 1 (2015) 54-61.
[13] S.G. Lim, R.W. Park, S.J. Shin, D. Yoon, J.K. Kang, J.C. Hwang, S.S. Kim, J.H. Kim, K.M. Lee, The relationship between the failure to eradicate Helicobacter pylori and previous antibiotics use, Digestive and Liver Disease 48(4) (2016) 385-390.
[14] M. Zamani, F. Ebrahimtabar, V. Zamani, W.H. Miller, R. Alizadeh-Navaei, J. Shokri-Shirvani, M.H. Derakhshan, Systematic review with meta-analysis: the worldwide prevalence of Helicobacter pylori infection, Aliment Pharm Ther 47(7) (2018) 868-876.
[15] I.C. Gonçalves, P.C. Henriques, C.L. Seabra, M.C. Martins, The potential utility of chitosan micro/nanoparticles in the treatment of gastric infection, Expert Review Anti-Infective Therapy 12(8) (2014) 981-92.
[16] M. Safavi, R. Sabourian, A. Foroumadi, Treatment of Helicobacter pylori infection: Current and future insights, World Journal of Clinical Cases 4(1) (2016) 5-19.
[17] S.Y. Kim, D.J. Choi, J. Chung, Antibiotic treatment for Helicobacter pylori : Is the end coming?, World Journal of Gastrointestinal Pharmacology and Therapeutics 6(4) (2015) 183-198.
[18] T. Niaz, A. Ihsan, R. Abbasi, S. Shabbir, T. Noor, M. Imran, Chitosan-albumin based core shell-corona nano-antimicrobials to eradicate resistant gastric pathogen, International Journal of Biological Macromolecules 138 (2019) 1006-1018.
[19] S. Devi, E. Rajakumara, N. Ahmed, Induction of Mincle by Helicobacter pylori and consequent anti-inflammatory signaling denote a bacterial survival strategy, Scientific Reports 5 (2015) 15049.

[20] A. Magalhaes, R. Marcos-Pinto, A.V. Nairn, M. Dela Rosa, R.M. Ferreira, S. Junqueira-Neto, D. Freitas, J. Gomes, P. Oliveira, M.R. Santos, N.T. Marcos, W. Xiaogang, C. Figueiredo, C. Oliveira, M. Dinis-Ribeiro, F. Carneiro, K.W. Moremen, L. David, C.A. Reis, Helicobacter pylori chronic infection and mucosal inflammation switches the human gastric glycosylation pathways, Biochimica et Biophysica Acta (BBA) - Molecular Basis of Disease 1852(9) (2015) 1928-39.
[21] C.Y. Kao, B.S. Sheu, J.J. Wu, Helicobacter pylori infection: An overview of bacterial virulence factors and pathogenesis, Biomedical Journal 39(1) (2016) 14-23.
[22] M. Amieva, R.M. Peek, Jr., Pathobiology of Helicobacter pylori-Induced Gastric Cancer, Gastroenterology 150(1) (2016) 64-78.
[23] B. Menchicchi, E. Savvaidou, C. Thöle, A. Hensel, F.M. Goycoolea, Low-Molecular-Weight Dextran Sulfate Nanocapsules Inhibit the Adhesion of Helicobacter pylori to Gastric Cells, ACS Applied Bio Materials 2(11) (2019) 4777-4789.
[24] S. Ramteke, N. Ganesh, S. Bhattacharya, N.K. Jain, Amoxicillin, clarithromycin, and omeprazole based targeted nanoparticles for the treatment of H. pylori, Journal of Drug Targeting 17(3) (2009) 225-34.
[25] Z. Wu, J. Hou, Y. Wang, M. Chai, Y. Xiong, W. Lu, J. Pan, Preparation and evaluation of amoxicillin loaded dual molecularly imprinted nanoparticles for anti-Helicobacter pylori therapy, International Journal of Pharmaceutics 496(2) (2015) 1006-14.
[26] S.K. Dey, P.K. De, A. De, S. Ojha, R. De, A.K. Mukhopadhyay, A. Samanta, Floating mucoadhesive alginate beads of amoxicillin trihydrate: A facile approach for H. pylori eradication, International Journal of Biological Macromolecules 89 (2016) 622-31.
[27] N.A. Thombre, P.S. Gide, Floating-bioadhesive gastroretentive Caesalpinia pulcherrima-based beads of amoxicillin trihydrate for Helicobacter pylori eradication, Drug Delivery 23(2) (2016) 405-19.
[28] A.O. Adebisi, B.R. Conway, Lectin-conjugated microspheres for eradication of Helicobacter pylori infection and interaction with mucus, International Journal of Pharmaceutics 470(1-2) (2014) 28-40.
[29] Y.H. Lin, S.C. Tsai, C.H. Lai, C.H. Lee, Z.S. He, G.C. Tseng, Genipin-cross-linked fucose-chitosan/heparin nanoparticles for the eradication of Helicobacter pylori, Biomaterials 34(18) (2013) 4466-79.
[30] M. Luo, Y.Y. Jia, Z.W. Jing, C. Li, S.Y. Zhou, Q.B. Mei, B.L. Zhang, Construction and optimization of pH-sensitive nanoparticle delivery system containing PLGA and UCCs-2 for targeted treatment of Helicobacter pylori, Colloids Surfaces B Biointerfaces 164 (2018) 11-19.
[31] S. Hao, Y. Wang, B. Wang, Q. Zou, H. Zeng, X. Chen, X. Liu, J. Liu, S. Yu, A novel gastroretentive porous microparticle for anti-Helicobacter pylori therapy: preparation, in vitro and in vivo evaluation, International Journal of Pharmaceutics 463(1) (2014) 10-21.
[32] Y. Lin, J. Lin, S. Chou, S. Chang, C. Chung, Y. Chen, C. Chang, Berberine-loaded targeted nanoparticles as specific Helicobacter pylori eradication therapy: in vitro and in vivo study, Nanomedicine 10(1) (2015).
[33] P. Li, X. Chen, Y. Shen, H. Li, Y. Zou, G. Yuan, P. Hu, H. Hu, Mucus penetration enhanced lipid polymer nanoparticles improve the eradication rate of Helicobacter pylori biofilm, Journal of Controlled Release 300 (2019) 52-63.
[34] P. Parreira, M. Fatima Duarte, C.A. Reis, M.C. Martins, Helicobacter pylori infection: A brief overview on alternative natural treatments to conventional therapy, Critical Reviews in Microbiology 42(1) (2014).
[35] G. Ayala, W.I. Escobedo-Hinojosa, C.F. de la Cruz-Herrera, I. Romero, Exploring alternative treatments for Helicobacter pylori infection, World Journal of Gastroenterology 20(6) (2014) 1450-69.
[36] C.L. Seabra, C. Nunes, M. Gomez-Lazaro, M. Correia, J.C. Machado, I.C. Gonçalves, C.A. Reis, S. Reis, M.C.L. Martins, Docosahexaenoic acid loaded lipid

nanoparticles with bactericidal activity against Helicobacter pylori, International Journal of Pharmaceutics 519(1-2) (2017) 128-137.
[37] C.L. Seabra, C. Nunes, M. Bras, M. Gomez-Lazaro, C.A. Reis, I.C. Goncalves, S. Reis, M.C.L. Martins, Lipid nanoparticles to counteract gastric infection without affecting gut microbiota, European Journal of Pharmaceutics and Biopharmaceutics 127 (2018).
[38] M.F. Garro, A.G. Salinas Ibanez, A.E. Vega, A.C. Arismendi Sosa, L. Pelzer, J.R. Saad, A.O. Maria, Gastroprotective effects and antimicrobial activity of Lithraea molleoides and isolated compounds against Helicobacter pylori, Journal of Ethnopharmacology 176 (2015) 469-74.
[39] W.I. Hinojosa, M.A. Quiroz, I.R. Alvarez, P.E. Castaneda, M.L. Villarreal, A.C. Taketa, Anti-Helicobacter pylori, gastroprotective, anti-inflammatory, and cytotoxic activities of methanolic extracts of five different populations of Hippocratea celastroides collected in Mexico, Journal of Ethnopharmacology 155(2) (2014) 1156-63.
[40] M.O. Makobongo, J.J. Gilbreath, D.S. Merrell, Nontraditional therapies to treat Helicobacter pylori infection, Journal of Microbiology 52(4) (2014) 259-72.
[41] B. Menchicchi, A. Hensel, F.M. Goycoolea, Polysaccharides as Bacterial Antiadhesive Agents and "Smart" Constituents for Improved Drug Delivery Systems Against Helicobacter pylori Infection, Current Pharmaceutical Design 21(33) (2015) 4888-906.
[42] Y. Gong, L. Tao, F. Wang, W. Liu, L. Jing, D. Liu, S. Hu, Y. Xie, N. Zhou, Chitosan as an adjuvant for a Helicobacter pylori therapeutic vaccine, Molecular Medicine Reports 12(3) (2015) 4123-32.
[43] M. Zeng, X. Mao, J. Li, W. Tong, B. Wang, Y. Zhang, G. Guo, Z. Zhao, L. Li, D. Wu, D. Lu, Z. Tan, H. Liang, C. Wu, D. Li, P. Luo, H. Zeng, W. Zhang, J. Zhang, B. Guo, F. Zhu, Q. Zou, Efficacy, safety, and immunogenicity of an oral recombinant Helicobacter pylori vaccine in children in China: a randomised, double-blind, placebo-controlled, phase 3 trial, The Lancet 386(10002) (2015) 1457-1464.
[44] A.M. Svennerholm, A. Lundgren, Progress in vaccine development against Helicobacter pylori, FEMS Immunology & Medical Microbiology 50(2) (2007) 146-56.
[45] S.J. Czinn, T. Blanchard, Vaccinating against Helicobacter pylori infection, Nature Reviews Gastroenterology & Hepatology 8(3) (2011) 133-40.
[46] M. Kong, X.G. Chen, K. Xing, H.J. Park, Antimicrobial properties of chitosan and mode of action: a state of the art review, International Journal of Food Microbiology 144(1) (2010) 51-63.
[47] R. Hejazi, M. Amiji, Chitosan-based gastrointestinal delivery systems, Journal of Controlled Release 89(2) (2003) 151-165.
[48] S. Dhawan, A.K. Singla, V.R. Sinha, Evaluation of Mucoadhesive Properties of Chitosan Microspheres Prepared by Different Methods, AAPS PharmSciTech 5(4) (2004).
[49] M. Fernandes, I.C. Goncalves, S. Nardecchia, I.F. Amaral, M.A. Barbosa, M.C. Martins, Modulation of stability and mucoadhesive properties of chitosan microspheres for therapeutic gastric application, International Journal of Pharmaceutics 454(1) (2013) 116-24.
[50] P. He, S.S. Davis, L. Illum, In vitro evaluation of the mucoadhesive properties of chitosan microspheres, International Journal of Pharmaceutics 166 (1998) 75–68.
[51] C. Lehr, J.A. Bouwstra, E.H. Schacht, H.E. Junginger, In vitro evaluation of mucoadhesive properties of chitosan and some other natural polymers, International Journal of Pharmaceutics 78 (1992) 43-48.
[52] S. Hirano, N. Nagao, Effects of Chitosan, Pectic Acid, Lysozyme, and Chitinase on the Growth of Several Phytopathogens, Agricultural and Biological Chemistry 53(11) (1989) 3065-3066.
[53] Y. Jiao, X. Pang, M. Liu, B. Zhang, L. Li, G. Zhai, Recent progresses in bioadhesive microspheres via transmucosal administration, Colloids Surfaces B 140 (2016) 361-72.

[54] D. Luo, J. Guo, F. Wang, J. Sun, G. Li, X. Cheng, M. Chang, X. Yan, Preparation and evaluation of anti-Helicobacter pylori efficacy of chitosan nanoparticles in vitro and in vivo, Journal of Biomaterials Science, Polymer Edition 20(11) (2009) 1587-96.
[55] F. Nogueira, I.C. Goncalves, M.C. Martins, Effect of gastric environment on Helicobacter pylori adhesion to a mucoadhesive polymer, Acta Biomaterialia 9(2) (2013) 5208-15.
[56] I.C. Gonçalves, A. Magalhães, M. Fernandes, I.V. Rodrigues, C.A. Reis, M.C. Martins, Bacterial-binding chitosan microspheres for gastric infection treatment and prevention, Acta Biomaterialia 9(12) (2013) 9370-8.
[57] I.C. Gonçalves, A. Magalhães, A.M. Costa, J.R. Oliveira, P.C. Henriques, P. Gomes, C.A. Reis, M.C. Martins, Bacteria-targeted biomaterials: Glycan-coated microspheres to bind Helicobacter pylori, Acta Biomaterialia 33 (2016) 40-50.
[58] M.R. Amieva, E.M. El-Omar, Host-bacterial interactions in Helicobacter pylori infection, Gastroenterology 134(1) (2008) 306-23.
[59] J.R. Oliveira, M.C.L. Martins, L. Mafra, P. Gomes, Synthesis of an O-alkynyl-chitosan and its chemoselective conjugation with a PEG-like amino-azide through click chemistry, Carbohydrate Polymers 87(1) (2012) 240-249.
[60] I.F. Amaral, P.L. Granja, M.A. Barbosa, Chemical modification of chitosan by phosphorylation: an XPS, FT-IR and SEM study, Journal of Biomaterials Science, Polymer Edition 16(12) (2005) 1575-1593.
[61] J. Brugnerotto, J. Lizardi, F.M. Goycoolea, W. Arguelles-Monal, J. Desbrieres, M. Rinaudo, An infrared investigation in relation with chitin and chitosan characterization, Polymer 42(8) (2001) 3569-3580.
[62] A. Lee, J. O'Rourke, M.C. De Ungria, B. Robertson, G. Daskalopoulos, M.F. Dixon, A standardized mouse model of Helicobacter pylori infection: Introducing the Sydney strain, Gastroenterology 112(4) (1997) 1386-1397.
[63] J. Mahdavi, B. Sonden, M. Hurtig, F.O. Olfat, L. Forsberg, N. Roche, J. Angstrom, T. Larsson, S. Teneberg, K.A. Karlsson, S. Altraja, T. Wadstrom, D. Kersulyte, D.E. Berg, A. Dubois, C. Petersson, K.E. Magnusson, T. Norberg, F. Lindh, B.B. Lundskog, A. Arnqvist, L. Hammarstrom, T. Boren, Helicobacter pylori SabA adhesin in persistent infection and chronic inflammation, Science 297(5581) (2002) 573-8.
[64] P. Falk, K.A. Roth, T. Boren, T.U. Westblom, J.I. Gordon, S. Normark, An invitro adherence assay reveals that Helicobacter pylor exhibits cell lineage-specific tropism in the human gastric epithelium

(host-crobil lnteractlons/adheslns/glycoproteins/gastrlc epithelial cell biolgy), Proceedings of the National Academy of Sciences of the USA 90 (1993) 2035-2039.
[65] P. Parreira, A. Magalhaes, I.C. Goncalves, J. Gomes, R. Vidal, C.A. Reis, D.E. Leckband, M.C. Martins, Effect of surface chemistry on bacterial adhesion, viability, and morphology, Journal of Biomedical Materials Research A 99(3) (2011) 344-53.
[66] Biological evaluation of medical devices, Part 12, Sample preparation and reference materials, SO 10993-12, 2004.
[67] Biological evaluation of medical devices Part 5, Tests for in vitro cytotoxicity, ISO 10993-5, 2009.
[68] S.A. Miller, D.D. Dykes, H.F. Polesky, A simple salting out procedure for extracting DNA from human nucleated cells, Nucleic Acids Research 16(3) (1988).
[69] M. Hammar, T. Tyszkiewicz, T. Wadstrom, P.W. O'Toole, Rapid Detection of Helicobacter pylori in Gastric Biopsy Material by Polymerase Chain Reaction, Journal of Clinical Microbiology 30(1) (1992) 54-58.
[70] J.Y. Hou, L.N. Gao, F.Y. Meng, Y.L. Cui, Mucoadhesive microparticles for gastroretentive delivery: preparation, biodistribution and targeting evaluation, Marine Drugs 12(12) (2014) 5764-87.
[71] S. Thamphiwatana, W. Gao, M. Obonyo, L. Zhang, In vivo treatment of Helicobacter pylori infection with liposomal linolenic acid reduces colonization and

ameliorates inflammation, Proceedings of the National Academy of Sciences of the USA 111(49) (2014) 17600-5.
[72] N.R. Salama, G. Otto, L. Tompkins, S. Falkow, Vacuolating cytotoxin of Helicobacter pylori plays a role during colonization in a mouse model of infection, Infection and Immunity 69(2) (2001) 730-6.
[73] R.L. Ferrero, J. Thiberge, M. Huerre, A. Labigne, Immune Responses of Specific-Pathogen-Free Mice to Chronic Helicobacter pylori (Strain SS1) Infection, Infection and Immunity 66(4) (1998) 1349-1355.
[74] E. Touati, V. Michel, M. Correia, L. Menghini, S. Genovese, M. Curini, F. Epifano, Boropinic acid, a novel inhibitor of Helicobacter pylori stomach colonization, Journal of Antimicrobial Chemotherapy 64(1) (2009) 210-1.
[75] C.R. da Silva, V. Michel, S. Genovese, M.C. Prevost, F. Epifano, E. Touati, Anti-Helicobacter pylori activities of natural isopentenyloxycinnamyl derivatives from Boronia pinnata, Nature Product Communications 7(10) (2012) 1347-50.
[76] S. Salillas, M. Alias, V. Michel, A. Mahia, A. Lucia, L. Rodrigues, J. Bueno, J.J. Galano-Frutos, H. De Reuse, A. Velazquez-Campoy, J.A. Carrodeguas, C. Sostres, J. Castillo, J.A. Ainsa, M.D. Diaz-de-Villegas, A. Lanas, E. Touati, J. Sancho, Design, Synthesis, and Efficacy Testing of Nitroethylene- and 7-Nitrobenzoxadiazol-Based Flavodoxin Inhibitors against Helicobacter pylori Drug-Resistant Clinical Strains and in Helicobacter pylori-Infected Mice, Journal of Medicinal Chemistry 62(13) (2019) 6102-6115.
[77] M. Correia, V. Michel, A.A. Matos, P. Carvalho, M.J. Oliveira, R.M. Ferreira, M.A. Dillies, M. Huerre, R. Seruca, C. Figueiredo, J.C. Machado, E. Touati, Docosahexaenoic acid inhibits Helicobacter pylori growth in vitro and mice gastric mucosa colonization, Plos One 7(4) (2012) e35072.
[78] S.I. Smith, K.S. Oyedeji, A.O. Arigbabu, F. Cantet, F. Megraud, O.O. Ojo, A.O. Uwaifo, J.A. Otegbayo, S.O. Ola, A.O. Coker, Comparison of three PCR methods for detection of Helicobacter pylori DNA and detection of cagA gene in gastric biopsy specimens, World Journal of Gastroenteroly 10(13) (2004) 1958-1960.
[79] P.M. Treuting, M.A. Valasek, S.M. Dintzis, Comparative Anatomy and Histology: A Mouse and Human Atlas. , 2012, pp. 155-175.
[80] X. Cai, J. Carlson, C. Stoicov, H. Li, T.C. Wang, J. Houghton, Helicobacter felis Eradication Restores Normal Architecture and Inhibits Gastric Cancer Progression in C57BL/6 Mice, Gastroenterology 128(7) (2005) 1937-1952.
[81] M. Rangel, J.C. Martins, A.N. Garcia, G.A. Conserva, A. Costa-Neves, C.L. Sant'Anna, L.R. de Carvalho, Analysis of the toxicity and histopathology induced by the oral administration of Pseudanabaena galeata and Geitlerinema splendidum (cyanobacteria) extracts to mice, Mar Drugs 12(1) (2014) 508-24.
[82] R.R. Seeley, T.D. Stephans, P. Tate, Anatomy and Physiology., 7th Edition ed., McGraw-Hill Higher Education2006.
[83] F.-L. Mi, H.-W. Sung, S.-S. Shyu, C.-C. Su, C.-K. Peng, Synthesis and characterization of biodegradable TPP/genipin co-crosslinked chitosan gel beads, Polymer 44(21) (2003) 6521-6530.
[84] H. Takeuchi, H. Yamamoto, Y. Kawashima, Mucoadhesive nanoparticulate systems for peptide drug delivery Advanced Drug Delivery Reviews 47 (2001) 39–54.
[85] S.K. Lai, Y.Y. Wang, J. Hanes, Mucus-penetrating nanoparticles for drug and gene delivery to mucosal tissues, Advanced Drug Delivery Reviews 61(2) (2009) 158-71.
[86] L.M. Ensign, R. Cone, J. Hanes, Oral drug delivery with polymeric nanoparticles: the gastrointestinal mucus barriers, Advanced Drug Delivery Reviews 64(6) (2012) 557-70.
[87] S.K. Lai, D.E. O'Hanlon, S. Harrold, S.T. Man, Y.Y. Wang, R. Cone, J. Hanes, Rapid transport of large polymeric nanoparticles in fresh undiluted human mucus, P Natl Acad Sci USA 104(5) (2007) 1482-1487.

[88] M.A. Elgadir, M.S. Uddin, S. Ferdosh, A. Adam, A.J.K. Chowdhury, M.Z.I. Sarker, Impact of chitosan composites and chitosan nanoparticle composites on various drug delivery systems: A review, Journal of Food and Drug Analysis 23(4) (2015) 619-629.
[89] S. Arora, S. Gupta, R.K. Narang, R.D. Budhiraja, Amoxicillin loaded chitosan-alginate polyelectrolyte complex nanoparticles as mucopenetrating delivery system for H. pylori, Scientific Pharmaceutics 79(3) (2011) 673-94.
[90] A. Sadio, J.K. Gustafsson, B. Pereira, C.P. Gomes, G.C. Hansson, L. David, A.P. Pego, R. Almeida, Modified-Chitosan/siRNA Nanoparticles Downregulate Cellular CDX2 Expression and Cross the Gastric Mucus Barrier, Plos One 9(6) (2014).
[91] D.E. Chickering, J.S. Jacob, T.A. Desai, M. Harrison, W.P. Harris, C.N. Morrell, P. Chaturvedi, E. Mathiowitz, Bioadhesive microspheres: III. An in vivo transit and bioavailability study of drug-loaded alginate and poly(fumaric-co-sebacic anhydride) microspheres, Journal of Controlled Release 48 (1997) 35–46.
[92] E.I. Rabea, M.E.-T. Badawy, C.V. Stevens, G. Smagghe, W. Steurbaut, Chitosan as Antimicrobial Agent: Applications and Mode of Action, Biomacromolecules 4(6) (2003).
[93] R.A. Cone, Barrier properties of mucus, Advanced Drug Delivery Reviews 61(2) (2009) 75-85.
[94] M.M. Amiji, Tetracycline-containing Chitosan Microspheres for Local Treatment of Helicobacter pylori Infection, Cellulose 14(1) (2006) 3-14.
[95] S.E. Ladirat, H.A. Schols, A. Nauta, M.H. Schoterman, B.J. Keijser, R.C. Montijn, H. Gruppen, F.H. Schuren, High-throughput analysis of the impact of antibiotics on the human intestinal microbiota composition, Journal of Microbiological Methods 92(3) (2013) 387-97.
[96] I. Adamsson, C. Edlund, C.E. Nord, Impact of treatment of Helicobacter pylori on the normal gastrointestinal microflora, Clinical Microbiology and Infection 6(4) (2000) 175-177.

Graphical abstract